

# Top-quark FCNC decays, LFVs, lepton $g - 2$ , and $W$ mass anomaly with inert charged Higgses

Chuan-Hung Chen,<sup>1,2,\*</sup> Cheng-Wei Chiang,<sup>3,2,†</sup> and Chun-Wei Su<sup>3,‡</sup>

<sup>1</sup>*Department of Physics, National Cheng-Kung University, Tainan 70101, Taiwan*

<sup>2</sup>*Physics Division, National Center for Theoretical Sciences, Taipei 10617, Taiwan*

<sup>3</sup>*Department of Physics and Center for Theoretical Physics,  
National Taiwan University, Taipei 10617, Taiwan*

(Dated: January 18, 2023)

## Abstract

The observed flavor-changing neutral-current (FCNC) processes in the standard model (SM) arise from the loop diagrams involving the weak charged currents mediated by the  $W$ -gauge boson. Nevertheless, the top-quark FCNCs and lepton-flavor violating processes resulting from the same mechanism are highly suppressed. We investigate possible new physics effects that can enhance the suppressed FCNC processes, such as  $t \rightarrow q(h, V)$  with  $V = \gamma, Z, g$ ,  $h \rightarrow \ell\ell'$ , and  $\ell \rightarrow \ell'\gamma$ . To achieve the assumption that the induced-FCNCs are all from quantum loops, we consider the scotogenic mechanism, where a  $Z_2$  symmetry is introduced and only new particles carry an odd  $Z_2$  parity. With the extension of the SM to include an inert Higgs doublet, an inert charged Higgs singlet, a vector-like singlet quark, and two neutral leptons, it is found that, with relevant constraints taken into account, the  $t \rightarrow c(h, Z)$ ,  $h \rightarrow \mu\tau$ , and  $\tau \rightarrow \ell\gamma$  decays can be enhanced up to the expected sensitivities in experiments. The branching ratios of  $h \rightarrow \mu^+\mu^-/\tau^+\tau^-$  from only new physics effects can reach up to  $\mathcal{O}(10^{-3})$ . Intriguingly, the resulting muon  $g - 2$  can fit the combined data within  $2\sigma$  errors, whereas the electron  $g - 2$  can have either sign with a magnitude of  $\mathcal{O}(10^{-13} - 10^{-12})$ . In addition, we examine the oblique parameters in the model and find that the resulting  $W$ -mass anomaly observed by CDF II can be accommodated.

---

\*E-mail: physchen@mail.ncku.edu.tw

†E-mail: chengwei@phys.ntu.edu.tw

‡E-mail: r10222026@ntu.edu.tw

## I. INTRODUCTION

While flavor-changing processes at tree level in the standard model (SM) arise from weak charged currents mediated by the  $W$  gauge boson, flavor-changing neutral currents (FCNCs) occur only via quantum loops and have been observed in various experiments, notably  $P - \bar{P}$  mixing and  $P \rightarrow P' \ell^+ \ell^-$  decays with  $P^{(\prime)}$  being the  $K$ ,  $D$ , and  $B$  mesons. However, not all loop-induced FCNC processes in the SM are sufficiently sizable and detectable under current experimental sensitivities. For instance, due to the Glashow-Iliopoulos-Maiani (GIM) mechanism [1], the top-quark FCNCs are highly suppressed, and the branching ratios (BRs) for the  $t \rightarrow q(g, \gamma, Z, h)$  decays with  $q = u, c$  are of the order of  $10^{-12} - 10^{-17}$  [2–4]. A similar suppression also happens in lepton flavor-violating (LFV) processes, e.g.,  $\ell \rightarrow \ell' \gamma$ ,  $\ell \rightarrow 3 \ell'$ , and  $h \rightarrow \ell \ell'$ .

The expected sensitivities in the high-luminosity (HL) LHC with an integrated luminosity of  $3 \text{ ab}^{-1}$  at  $\sqrt{s} = 14 \text{ TeV}$  are expected to reach  $\mathcal{O}(10^{-5})$  for  $t \rightarrow qZ/q\gamma$ ,  $\mathcal{O}(10^{-4})$  for  $t \rightarrow qh$  [5], and  $\mathcal{O}(10^{-4})$  for  $h \rightarrow e\tau/\mu\tau$  [6]. In addition, the  $\mu \rightarrow e\gamma$  decay in MEG II experiment can reach the sensitivity of  $6 \times 10^{-14}$  [7], and  $\tau \rightarrow e\gamma/\mu\gamma$  can be probed at the level of  $\mathcal{O}(10^{-9})$  in Belle II [8]. Thus, if any signal in these processes is detected in experiments, it definitely indicates new physics effects at play. Some interesting extensions of the SM proposed to enhance the top-FCNC decays can be found in Refs. [9–28].

A long-standing anomaly in the muon anomalous magnetic dipole moment (muon  $g - 2$ ) observed at BNL [29] is now supported by the recent new measurement performed in the E989 Run 1 experiment at Fermilab [30]. The combined data shows a  $4.2\sigma$  deviation from the SM prediction, which is obtained by the data-driven evaluations of hadronic vacuum polarization (HVP):

$$\Delta a_\mu = a_\mu^{\text{exp}} - a_\mu^{\text{SM}} = (2.51 \pm 0.50) \times 10^{-9}. \quad (1)$$

We note that although the discrepancy in Eq. (1) could possibly be narrowed down according to a lattice calculation QCD [31, 32], the tension between theoretical estimates and data has not been completely resolved yet. In addition, using precision measurements of the fine structure constant, electron  $g - 2$  measured separately using cesium [33] and rubidium [34]

atoms is respectively given by:

$$\begin{aligned}\Delta a_e(\text{Cs}) &= (-8.8 \pm 3.6) \times 10^{-13}, \\ \Delta a_e(\text{Rb}) &= (4.8 \pm 3.0) \times 10^{-13}.\end{aligned}\tag{2}$$

Further precision measurement needs to be done in order to resolve the above discrepancy and to tell us whether the data agree with the SM prediction. In any case, a significant deviation from the SM prediction in lepton  $g - 2$  is an important channel to probe new physics effects in the lepton sector [35–61].

Using the full dataset of the integrated luminosity of  $8.8 \text{ fb}^{-1}$  in proton-antiproton collisions at  $\sqrt{s} = 1.96 \text{ TeV}$ , the CDF II Collaboration recently reported the measured mass of  $W$  gauge boson as:

$$m_W = 80.4335 \pm 0.0094 \text{ GeV},\tag{3}$$

where the observed value is different from  $m_W = 80.370 \pm 0.019 \text{ GeV}$  measured by ATLAS [63] and earlier result of  $m_W = 80.385 \pm 0.015 \text{ GeV}$  that is the measurement of LEP combined with Tevatron [64]. Moreover, the new observation has a  $7\sigma$  deviation from the SM prediction  $m_W = 80.361 \text{ GeV}$  [65]. If the  $W$ -mass anomaly is confirmed by the measurements at the LHC with more cumulative data, it would be a solid piece of evidence that exhibits the effects of new physics [66–79].

In this work, we investigate a new physics model that can enhance the top-FCNC and LFV processes, up to the experimental sensitivities mentioned above. Furthermore, we will show that, after all possible constraints being taken into account, these new physics effects can lead to  $\Delta a_\mu$  of  $\mathcal{O}(10^{-9})$  and  $|\Delta a_e|$  of  $\mathcal{O}(10^{-13} - 10^{-12})$  and explain the  $W$ -mass anomaly.

Note that the  $t \rightarrow q(h, Z)$  and  $h \rightarrow \ell\ell'$  decays can in general proceed via tree-level diagrams through mixing. Such tree-level effects can be naturally suppressed when the new particles are charged under an unbroken symmetry, for which the SM particles remain neutral. Under the latter scenario, we consider in this study a SM extension where all FCNCs arise only from loop diagrams. To achieve the purpose, we impose a  $Z_2$  symmetry under which the new and SM particles can be classified as  $Z_2$ -odd and -even, respectively. From the initial- and final-state particles involved in the above-mentioned processes, one can infer that the new mediating particles running in the loop diagrams should be  $Z_2$ -odd scalar bosons and  $Z_2$ -odd fermions.

In order to realize the above inference based on a gauge anomaly-free model, a minimal extension to the SM includes one inert Higgs doublet [80], one charged Higgs singlet [81], one  $SU(2)_L$ -singlet vector-like quark [28], and two singlet vector-like Dirac-type neutral leptons [82], where the  $Z_2$ -odd quark is responsible for the top-FCNC processes, and the  $Z_2$ -odd singlet leptons are for the rare lepton flavor-conserving and -violating processes. The new singlet  $Z_2$ -odd charged Higgs boson can be used to enhance the rare decays and avoid the chirality suppression of  $m_F/\Lambda$ , where  $m_F$  is the mass of the SM particle and  $\Lambda$  is the mass scale of heavy particle in the model.

There are three scalar bosons in the inert Higgs doublet, namely, an inert charged Higgs, a scalar, and a pseudoscalar, with the lightest neutral inert scalar being a possible DM candidate. It is found that the top-FCNC and LFV processes are dominated by the charged Higgs boson. Since fermions of different chiralities couple to different charged Higgs bosons in the model, the chirality-flipping processes  $t \rightarrow q(h, \gamma)$ ,  $h \rightarrow \ell\ell'$ , and  $\ell \rightarrow \ell'\gamma$  strongly depend on the mixing of the two charged Higgs bosons. Furthermore, because of the charged Higgs mixing, the induced lepton  $g - 2$  can be either positive or negative, where the contribution from a single charged Higgs boson is usually negative at the one-loop level.

This paper is organized as follows: We introduce the model and derive the relevant gauge couplings, masses of inert scalars, charged Higgs mixing, and Yukawa couplings in Sec. II. The induced top-FCNC and LFV processes including lepton  $g - 2$  are studied in detail in Sec. III. In Sec. IV, we discuss the strict constraints from  $\Delta B(D) = 2$  transitions, the Higgs to diphoton decay, and the  $\mu \rightarrow e\gamma$  decay. In Sec. V, we comprehensively scan the parameter space by taking into account all major constraints. Finally, a summary of the work is given in Sec. VI.

## II. MODEL, GAUGE COUPLINGS, AND YUKAWA COUPLINGS

To enhance the suppressed FCNC processes in the SM and to explain the muon  $g - 2$  anomaly and  $W$ -mass excesses through loop effects, we extend the SM by including one inert Higgs doublet ( $H_I$ ), one charged scalar singlet ( $\chi^\pm$ ), two vector-like lepton singlet ( $N_{1,2}$ ), and one vector-like quark singlet ( $B$ ) under  $SU(2)_L$ . In order to obtain a stable dark matter (DM) candidate, we impose a  $Z_2$  symmetry in such a way that the new particles are  $Z_2$ -odd and the SM particles are  $Z_2$ -even. The representations and charge assignments of  $Z_2$ -odd



particles are given in Table I, where we use the convention that the electric charge of a field  $Q = I_3 + \frac{Y}{2}$  with  $I_3$  and  $Y$  being the isospin and hypercharge quantum numbers, respectively. Accordingly, we discuss the relevant couplings from the scalar potential, gauge sector, and Yukawa sector in the following subsections.

TABLE I: Representations and charge assignments of new fields.

	$SU(2)_L$	$U(1)_Y$	$Z_2$	Lepton
$H_I$	2	1	-1	0
$\chi^+$	1	2	-1	0
$N_{1,2}$	1	0	-1	1
$B$	1	-2/3	-1	0

### A. Inert charged Higgs mixing and trilinear Higgs couplings

With the addition of one inert Higgs doublet and one charged Higgs singlet into the SM, the most general scalar potential consistent with the required symmetries is given by:

$$\begin{aligned}
V = & \mu_1^2 H^\dagger H + \mu_2^2 H_I^\dagger H_I + \lambda_1 (H^\dagger H)^2 + \lambda_2 (H_I^\dagger H_I)^2 + \lambda_3 (H^\dagger H)(H_I^\dagger H_I) \\
& + \lambda_4 (H^\dagger H_I)(H_I^\dagger H) + \frac{1}{2}[\lambda_5 (H^\dagger H_I) + H.c.] + m_{\chi^\pm}^2 \chi^- \chi^+ \\
& + [\mu_\chi H_I^T i\tau_2 H \chi^- + H.c.] + \lambda_1^\chi (\chi^- \chi^+)^2 + \lambda_2^\chi H^\dagger H \chi^- \chi^+ + \lambda_3^\chi H_I^\dagger H_I \chi^- \chi^+, \quad (4)
\end{aligned}$$

where  $H$  is the SM Higgs doublet,  $\mu_\chi$  has the dimension of mass, and  $\tau_2$  is the second Pauli matrix. To examine the spectra of scalar bosons, we write the components of the scalar doublets as:

$$H = \begin{pmatrix} G^+ \\ \frac{1}{\sqrt{2}}(v + h + iG^0) \end{pmatrix}, \quad H_I = \begin{pmatrix} H_I^+ \\ \frac{1}{\sqrt{2}}(S_I + iA_I) \end{pmatrix}, \quad (5)$$

where  $\mu_1^2 < 0$  is assumed to facilitate spontaneous electroweak symmetry breaking (EWSB),  $G^{\pm,0}$  are the Goldstone bosons,  $v$  is the vacuum expectation value (VEV) of  $H$ , and  $h$  is the SM Higgs boson. Note that the components in these two doublet fields do not mix due to the imposed  $Z_2$  symmetry. Moreover, we take  $\mu_2^2, m_\chi^2 > 0$  so that  $S_I$  ( $A_I$ ),  $H_I^\pm$ , and  $\chi^\pm$  are massive particles before EWSB.

In addition to the tadpole conditions, i.e.,  $\partial V/\partial h(S_I) = 0$ , the vacuum stability is controlled by the co-positivity criteria of the dimension-4 terms in Eq. (4) and lead to [84–86]:

$$\begin{aligned} \lambda_{1,2}, \lambda_{1,2,3}^\chi &\geq 0, \quad \lambda_2^\chi + 2\sqrt{\lambda_1\lambda_1^\chi} > 0, \quad \lambda_3^\chi + 2\sqrt{\lambda_2\lambda_1^\chi} > 0, \\ \lambda_3 + 2\sqrt{\lambda_1\lambda_2} &\geq 0, \quad \lambda_3 + \lambda_4 - |\lambda_5| + 2\sqrt{\lambda_1\lambda_2} \geq 0. \end{aligned} \quad (6)$$

On the other hand, the tree-level perturbative unitarity of scalar scattering amplitudes requires that  $|\lambda_i|, |\lambda_i^\chi| \leq 4\pi$  [87].

With the parametrization in Eq. (5), the masses of  $S_I$  and  $A_I$  are given by:

$$m_{S_I}^2 = \mu_2^2 + \frac{\lambda_L v^2}{2}, \quad m_{A_I}^2 = \mu_2^2 + \frac{\lambda_A v^2}{2}, \quad (7)$$

with  $\lambda_{L(A)} \equiv \lambda_3 + \lambda_4 \pm \lambda_5$ . The two  $Z_2$ -odd charged Higgs bosons in the model can mix through the dimension-3 term  $\mu_\chi H_I^T i\tau_2 H \chi^-$  and, therefore, has the mass-square matrix

$$\begin{aligned} (H_I^-, \chi^-) &\begin{pmatrix} m_{11}^2 & m_{12}^2 \\ m_{12}^2 & m_{22}^2 \end{pmatrix} \begin{pmatrix} H_I^+ \\ \chi^+ \end{pmatrix}, \\ \text{with } m_{11}^2 &= \mu_2^2 + \frac{\lambda_3 v^2}{2}, \quad m_{12}^2 = \frac{\mu_\chi v}{\sqrt{2}}, \quad m_{22}^2 = \mu_\chi^2 + \frac{\lambda_2^\chi v^2}{2}. \end{aligned} \quad (8)$$

Suppose this  $2 \times 2$  real symmetric mass-square matrix is diagonalized by an  $SO(2)$  orthogonal rotation defined by

$$\begin{pmatrix} H_1^+ \\ H_2^+ \end{pmatrix} = \begin{pmatrix} c_{\theta_\chi} & c_{\theta_\chi} \\ -s_{\theta_\chi} & c_{\theta_\chi} \end{pmatrix} \begin{pmatrix} H_I^+ \\ \chi^+ \end{pmatrix} \quad (9)$$

where  $c_{\theta_\chi} \equiv \cos \theta_\chi$  and  $s_{\theta_\chi} \equiv \sin \theta_\chi$ . Then we obtain the mass eigenvalues and the mixing angle as:

$$\begin{aligned} m_{1(2)}^2 &= \frac{m_{11}^2 + m_{22}^2}{2} \pm \frac{1}{2} \sqrt{(m_{22}^2 - m_{11}^2)^2 + 4(m_{12}^2)^2}, \\ s_{2\theta_\chi} &= -\frac{2m_{12}^2}{m_2^2 - m_1^2}, \end{aligned} \quad (10)$$

where  $s_{2\theta_\chi} \equiv \sin 2\theta_\chi$ .

Since the  $t \rightarrow qh$  and  $h \rightarrow \ell\ell'$  processes involve the Higgs couplings to the  $Z_2$ -odd scalars, we need to extract the trilinear Higgs couplings to  $H_{1,2}^\pm$ ,  $S_I$ , and  $A_I$  from the scalar potential. According to Eqs. (4) and (9), the  $h$ - $H_i^-$ - $H_i^+$  and  $h$ - $S_I$ - $A_I$  interactions

can be written as:

$$\begin{aligned}
\mathcal{L}_{h\phi_i\phi_j} &= -\lambda_{ij}^h v h H_i^- H_j^+ - \frac{1}{2} \lambda_L v h (S_I^2 + A_I^2), \\
\lambda_{11}^h &= \lambda_3 c_{\theta_\chi}^2 + \lambda_2^\chi s_{\theta_\chi}^2 - \frac{m_{H_2^\pm}^2 - m_{H_1^\pm}^2}{2v^2} s_{2\theta_\chi}^2, \\
\lambda_{22}^h &= \lambda_3 s_{\theta_\chi}^2 + \lambda_2^\chi c_{\theta_\chi}^2 + \frac{m_{H_2^\pm}^2 - m_{H_1^\pm}^2}{2v^2} s_{2\theta_\chi}^2, \\
\lambda_{12}^h &= \frac{-\lambda_3 + \lambda_2^\chi}{2} s_{2\theta_\chi} - \frac{m_{H_2^\pm}^2 - m_{H_1^\pm}^2}{2v^2} c_{2\theta_\chi} s_{2\theta_\chi}, \\
\lambda_L &= \lambda_3 + \lambda_4 + \lambda_5.
\end{aligned} \tag{11}$$

Here, according to Eq. (10), we have used the mixing angle  $\theta_\chi$  instead of  $\mu_\chi$ .

## B. Gauge couplings to the $Z_2$ -odd particles

To study the  $t \rightarrow q(\gamma, Z)$  and  $\ell \rightarrow \ell' \gamma$  processes, which arise from  $\gamma$ - and  $Z$ -penguin diagrams mediated by  $H_{1,2}^\pm$  and  $S_I(A_I)$  in the loops, we need to know the gauge couplings to these scalars. The kinetic terms of  $H_I$  and  $\chi^\pm$  in the  $SU(2)_L \times U(1)_Y$  gauge symmetry are written by

$$\mathcal{L}_{\text{kin}} \supset (D_\mu H_I)^\dagger D^\mu H_I + (D_\mu \chi^+)^\dagger D^\mu \chi^+, \tag{12}$$

where the covariant derivatives of the scalar fields are given by:

$$\begin{aligned}
D_\mu H_I &= \left( \partial_\mu + i \frac{g}{2} \vec{\tau} \cdot \vec{W}_\mu + i \frac{g'}{2} B_\mu \right) H_I, \\
D_\mu \chi^+ &= (\partial_\mu + i g' B_\mu) \chi^+.
\end{aligned} \tag{13}$$

If we parametrize the photon and  $Z$ -gauge boson states as

$$\begin{aligned}
A_\mu &= c_W B_\mu + s_W W_\mu^3, \\
Z_\mu &= -s_W B_\mu + c_W W_\mu^3,
\end{aligned} \tag{14}$$

with  $c_W(s_W) = \cos \theta_W(\sin \theta_W)$  and  $\theta_W$  being the Weinberg's angle, the gauge couplings to  $H_i^\pm$ ,  $S_I$ , and  $A_I$  are obtained as:

$$\begin{aligned}
\mathcal{L}_{\gamma, Z, W^\pm} &\supset ie A^\mu \sum_{i=1}^2 (\partial_\mu H_i^- H_i^+ - H_i^- \partial_\mu H_i^+) \\
&\quad + i \frac{g}{2c_W} c_{ij}^Z Z^\mu (\partial_\mu H_i^- H_j^+ - H_i^- \partial_\mu H_j^+) - \frac{g}{2c_W} Z^\mu (\partial_\mu A_I H_I - A_I \partial_\mu H_I) \\
&\quad + i \frac{g \xi_i}{\sqrt{2}} W^{+\mu} [(\partial_\mu H_i^- (S_I + i A_I) - H_i^- \partial_\mu (S + i A_I)) + \text{H.c.}] ,
\end{aligned} \tag{15}$$

where  $\xi_1 = c_{\theta_\chi}$ ,  $\xi_2 = -s_{\theta_\chi}$ , and the coefficients  $c_{ij}^Z$  are given by

$$c_{11}^Z = c_{\theta_\chi}^2 - 2s_W^2, \quad c_{12}^Z = c_{21}^Z = c_{\theta_\chi} s_{\theta_\chi}, \quad c_{22}^Z = s_{\theta_\chi}^2 - 2s_W^2. \quad (16)$$

In addition to the emission from  $H_i^\pm$  and  $S_I(A_I)$ , the photon and  $Z$ -gauge boson can be emitted from the  $B$  quark in the loop diagrams. If we write the covariant derivative of  $B$  quark to be  $D_\mu B = (\partial_\mu + ig' Q_B B_\mu)B$ , the gauge couplings of the  $B$  quark are given by:

$$\mathcal{L}_{VBB} = -e Q_B \bar{B} \gamma_\mu B A^\mu + \frac{g Q_B s_W^2}{c_W} \bar{B} \gamma_\mu B Z^\mu. \quad (17)$$

Since  $B$  is a  $SU(2)_L$  singlet, there is no charged-current interaction with the  $W$ -gauge boson.

### C. Yukawa couplings

In addition to the Higgs and gauge couplings, the Yukawa interactions of the SM fermions to  $Z_2$ -odd particles are also important for the rare FCNC processes. According to the representations and charge assignments of  $Z_2$ -odd particles, the relevant Yukawa interactions and mass term are:

$$\begin{aligned} -\mathcal{L}_Y = & \bar{L} Y^{\ell'} H \ell'_R + \overline{N_{kL}} \mathbf{y}_{1k}^\ell \ell'_R \chi^+ + \bar{L} \mathbf{y}_{2k}^\ell \widetilde{H}_I N_{kR} + \overline{B_L} \mathbf{y}_1^B u_R \chi^- \\ & + \overline{Q_L} \mathbf{y}_2^B H_I B_R + m_B \overline{B_L} \bar{B}_R + m_{N_k} \overline{N_{kL}} N_{kR} + \text{H.c.}, \end{aligned} \quad (18)$$

where we have suppressed the flavor indices,  $\mathbf{y}_{jk}^\ell$  and  $\mathbf{y}_j^B$  ( $j = 1, 2$ ) carry the lepton and quark flavors,  $L^T = (\nu_{\ell'}, \ell')_L$  and  $Q^T = (u, d)_L$  are the lepton and quark doublets in the SM, respectively, and  $\widetilde{H}_I \equiv i\tau_2 H_I^*$ . In terms of the physical states, the Yukawa couplings of fermions to  $H_i^\pm$  and  $S_I(A_I)$  can be written as:

$$\begin{aligned} -\mathcal{L}_Y \supset & \bar{u} (C_{BL}^i P_L + C_{BR}^i P_R) B H_i^+ + \bar{\ell} (C_{N_k L}^i P_L + C_{N_k R}^i P_R) N_k H_i^- \\ & + \frac{1}{\sqrt{2}} \bar{d} V_{\text{CKM}}^\dagger \mathbf{y}_2^B P_R B (S_I + iA_I) + \frac{1}{\sqrt{2}} \bar{\nu} \mathbf{y}_{2k}^\ell P_R N_k (S_I - iA_I) + \text{H.c.}, \end{aligned} \quad (19)$$

where the weak states of up-type quarks are chosen to align to their physical states,  $V_{\text{CKM}}$  is the Cabibbo-Kobayashi-Maskawa (CKM) matrix, and the couplings  $C_{BL, BR}^i$  and  $C_{N_k L, N_k R}^i$  are given by:

$$\begin{aligned} C_{BL}^1 &= \mathbf{y}_1^B s_{\theta_\chi}, \quad C_{BR}^1 = \mathbf{y}_2^B c_{\theta_\chi}, \quad C_{BL}^2 = \mathbf{y}_1^B c_{\theta_\chi}, \quad C_{BR}^2 = -\mathbf{y}_2^B s_{\theta_\chi}, \\ C_{N_k L}^1 &= \mathbf{y}_{1k}^\ell s_{\theta_\chi}, \quad C_{N_k R}^1 = -\mathbf{y}_{2k}^\ell c_{\theta_\chi}, \quad C_{N_k L}^2 = \mathbf{y}_{1k}^\ell c_{\theta_\chi}, \quad C_{N_k R}^2 = \mathbf{y}_{2k}^\ell s_{\theta_\chi}. \end{aligned} \quad (20)$$

### III. PHENOMENOLOGY

Based on the introduced interactions, we formulate in this section the expressions for the processes of interest, such as  $t \rightarrow q(h, \gamma, Z)$ ,  $h \rightarrow \ell\ell'$ , radiative lepton decays, lepton  $g - 2$ , and the oblique parameters, which can be related to the correction of  $W$  mass. We note that since the calculation for  $t \rightarrow qg$  is similar to that for  $t \rightarrow q\gamma$  and, by neglecting the small different factor, the branching ratio for  $t \rightarrow qg$  can be approximately estimated as:

$$BR(t \rightarrow qg) \sim \frac{\alpha_s}{\alpha} C_F BR(t \rightarrow q\gamma), \quad (21)$$

where  $C_F = 4/3$ ,  $\alpha = e^2/4\pi$ , and  $\alpha_s = g_s^2/4\pi$ . Using  $\alpha_s/\alpha \sim 14.2$ , it can be seen that the branching ratio of  $t \rightarrow qg$  is roughly one order of magnitude larger than that of  $t \rightarrow q\gamma$ . In the following, we just focus on the  $t \rightarrow q\gamma$  analysis.

#### A. Top-FCNC processes

In this subsection, we derive the loop-induced effective interactions for top-FCNC processes, where the current upper limits are shown in Table II. Because we only introduce a down-type  $B$  quark, from the Yukawa interactions in Eq. (19), it can be seen that the loop-induced top-FCNCs can only arise from the inert charged Higgses, where the Feynman diagrams are shown in Fig. 1. Since the photon couplings are Higgs-flavor diagonal,  $H_i^\pm = H_j^\pm$  for the  $\gamma$ -penguin in Fig. 1(a).

TABLE II: Experimental upper limits of  $t \rightarrow q(h, \gamma, Z)$  [94].

Channel	$t \rightarrow uh$	$t \rightarrow ch$	$t \rightarrow q\gamma$	$t \rightarrow qZ$
Exp. UL	$1.2 \times 10^{-3}$	$1.1 \times 10^{-3}$	$1.8 \times 10^{-4}$	$5 \times 10^{-4}$

In terms of the chiral structures of the initial- and final-state quarks, the effective interactions for  $t \rightarrow q(h, \gamma, Z)$  can be parametrized as [28]:

$$\begin{aligned} \mathcal{L}_{t \rightarrow q(h, \gamma, Z)} = & -C_L^h \bar{q} P_L t h - C_R^h \bar{q} P_R t h - \frac{1}{m_t} \bar{q} i \sigma_{\mu\nu} \epsilon_\gamma^{\mu*} k^\nu (B_L^\gamma P_L + B_R^\gamma P_R) t \\ & - \bar{q} \gamma_\mu (A_L^Z P_L + A_R^Z P_R) t Z^\mu - \frac{1}{m_t} \bar{q} i \sigma_{\mu\nu} \epsilon_Z^{\mu*} k^\nu (B_L^Z P_L + B_R^Z P_R) t, \end{aligned} \quad (22)$$

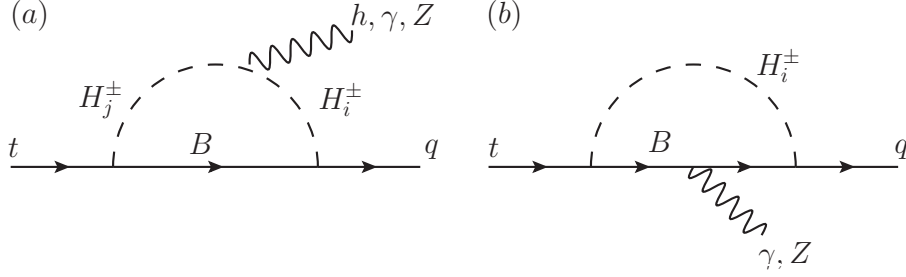


FIG. 1: Feynman diagrams for  $t \rightarrow q(h, \gamma, Z)$  induced by  $H_i^\pm$  and  $B$ .

where  $\epsilon_V$  denotes the polarization of a vector gauge boson. Using the introduced interactions, we can find the relations among the effective coefficients and the parameters in the model. The branching ratios of  $t \rightarrow q(h, \gamma, Z)$  are then given by:

$$\begin{aligned}
 Br(t \rightarrow q\gamma) &= \frac{m_t}{16\pi\Gamma_t} (|B_L^\gamma|^2 + |B_R^\gamma|^2) , \\
 Br(t \rightarrow qh) &= \frac{m_t}{32\pi\Gamma_t} \left(1 - \frac{m_h^2}{m_t^2}\right)^2 (|C_L^h|^2 + |C_R^h|^2) , \\
 Br(t \rightarrow qZ) &= \frac{1}{\Gamma_t} \frac{G_F m_t^3}{4\sqrt{2}\pi} \frac{c_W^2}{g^2} \left(1 - \frac{m_Z^2}{m_t^2}\right)^2 \sum_{\chi=L,R} \left[ |A_\chi^Z - B_{\chi'}^Z|^2 \left(1 + \frac{2m_Z^2}{m_t^2}\right) \right. \\
 &\quad \left. + (|B_\chi^Z|^2 + 2Re(A_\chi^Z - B_{\chi'}^Z)B_{\chi'}^{Z*}) \left(1 - \frac{m_Z^2}{m_t^2}\right) \right] , \quad (23)
 \end{aligned}$$

where  $\Gamma_t$  is the top-quark width, and  $\chi'$  has to be chosen to have the opposite chirality to  $\chi$ , i.e.,  $B_{\chi'}^Z = B_{R(L)}^Z$  when  $A_\chi^Z = A_{L(R)}^Z$ .

Since we focus on the scenario that  $m_B \sim \text{TeV}$  and  $m_{H_{I,\chi}} \sim \mathcal{O}(v)$ , for simplicity we neglect small factors, such as  $m_{H_i^\pm}^2/m_B^2$  and  $m_{t,h,Z}^2/m_B^2$ . As a result, the effective coefficients from Fig. 1(a) and (b) for  $t \rightarrow q\gamma$  are:

$$\begin{aligned}
 B_R^\gamma &\approx \sum_{i=1}^2 \frac{e(C_{BR}^i)_q(C_{BL}^i)_3}{(4\pi)^2} \sqrt{r_t} \left( J_\gamma^1(r_{H_i^\pm}, r_t, 0) - Q_B J_\gamma^2(r_{H_i^\pm}, r_t, 0) \right) , \\
 B_L^\gamma &\approx \sum_{i=1}^2 \frac{e(C_{BL}^i)_q(C_{BR}^i)_3}{(4\pi)^2} \sqrt{r_t} \left( J_\gamma^1(r_{H_i^\pm}, r_t, 0) - Q_B J_\gamma^2(r_{H_i^\pm}, r_t, 0) \right) ; \quad (24)
 \end{aligned}$$

those for  $t \rightarrow qh$  are:

$$\begin{aligned}
 C_R^h &\approx \frac{v}{(4\pi)^2 m_B} \sum_{i,j=1}^2 (C_{BL}^j)_3 \lambda_{ji}^h J_h(r_{H_i^\pm}, r_{H_j^\pm}, r_t, r_h) (C_{BR}^i)_q , \\
 C_L^h &\approx \frac{v}{(4\pi)^2 m_B} \sum_{i,j=1}^2 (C_{BR}^j)_3 \lambda_{ji}^h J_h(r_{H_i^\pm}, r_{H_j^\pm}, r_t, r_h) (C_{BL}^i)_q ; \quad (25)
 \end{aligned}$$

and those for  $t \rightarrow qZ$  are:

$$\begin{aligned}
B_R^Z &\approx \frac{g\sqrt{r_t}}{2c_W(4\pi)^2} \sum_{i,j=1}^2 (C_{BL}^j)_3 (C_{BR}^i)_q \left( c_{ji}^Z J_Z^1(r_{H_i^\pm}, r_{H_j^\pm}, r_t, r_Z) - 2s_W^2 Q_B \delta_{ij} J_\gamma^2(r_{H_i^\pm}, r_t, r_Z) \right), \\
B_L^Z &\approx \frac{g\sqrt{r_t}}{2c_W(4\pi)^2} \sum_{i,j=1}^2 (C_{BR}^j)_3 (C_{BL}^i)_q \left( c_{ji}^Z J_Z^1(r_{H_i^\pm}, r_{H_j^\pm}, r_t, r_Z) - 2s_W^2 Q_B \delta_{ij} J_\gamma^2(r_{H_i^\pm}, r_t, r_Z) \right), \\
A_R^Z &\approx \frac{gs_W^2 Q_B}{c_W(4\pi)^2} \sum_{i=1}^2 (C_{BL}^i)_3 (C_{BL}^i)_q J_Z^2(r_{H_i^\pm}, r_t, r_Z) + B_L^Z, \\
A_L^Z &\approx \frac{gs_W^2 Q_B}{c_W(4\pi)^2} \sum_{i=1}^2 (C_{BR}^i)_3 (C_{BR}^i)_q J_Z^2(r_{H_i^\pm}, r_t, r_Z) + B_R^Z;
\end{aligned} \tag{26}$$

where  $r_f \equiv m_f^2/m_B^2$ , and the loop integrals are defined as:

$$\begin{aligned}
J_\gamma^1(a, b, c) &= \int_0^1 dx_1 \int_0^{x_1} dx_2 \frac{1-x_1}{1-x_1+ax_1-bx_2(1-x_1)+cx_2^2}, \\
J_\gamma^2(a, b, c) &= \int_0^1 dx_1 \int_0^{x_1} dx_2 \frac{x_1}{x_1+a(1-x_1)-bx_2(1-x_1)+cx_2^2}, \\
J_h(a, b, c, d) &= \int_0^1 dx_1 \int_0^{x_1} dx_2 \frac{1}{1-(1-a)x_1+(b-a)x_2-cx_2(1-x_1)+dx_2^2}, \\
J_Z^1(a, b, c, d) &= \int_0^1 dx_1 \int_0^{x_1} dx_2 \frac{1-x_1}{1-(1-a)x_1+(b-a)x_2-cx_2(1-x_1)+dx_2^2}, \\
J_Z^2(a, b, c) &= \int_0^1 dx_1 \int_0^{x_1} dx_2 \frac{1}{x_1+a(1-x_1)-bx_2(1-x_1)+cx_2^2}.
\end{aligned} \tag{27}$$

With the limits  $a, b, c, d \ll 1$ , the loop integrals can be simplified to be:  $J_\gamma^1 \approx J_\gamma^2 \approx J_Z^1 \approx 1/2$  and  $J_Z^2 \approx 1$ . We note that the  $\sqrt{r_t} = m_t/m_B$  factor is retained, where the  $m_t$  does not arise from the mass insertion in the top-quark line but is used to fit the parametrization in Eq. (22).

Since the photon couplings to  $H_i^\pm$  are charged Higgs flavor diagonal, unlike the  $Z$  couplings to  $H_i^\pm$  which involve the  $Z$ - $H_1^\pm$ - $H_2^\mp$  interactions, we have  $B_{R,L}^\gamma \approx 0$  when the limit of  $m_{H_i^\pm}/m_B \approx 0$  is taken because of a strong cancellation between  $H_1^\pm$  and  $H_2^\pm$ . In addition, although  $B_{R,L}^Z$  in Eq. (26) can avoid the cancellation in the limit of  $m_{H_i^\pm}/m_B \approx 0$ , for  $c_{12}^Z$  and  $(C_{BR(BL)}^{1,2})_3 (C_{BL(BR)}^{2,1})_q$  all have  $\theta_\chi$  dependence and  $m_t/(2m_B) \sim s_W^2 Q_B$  for  $m_B \sim 1$  TeV,  $B_{R,L}^Z$  are smaller than other effective coefficients and lead to subleading effects. Therefore, it is the first term in  $A_{R(L)}^Z$  that makes the dominant contribution.

## B. Lepton flavor-conserving and -violating Higgs decays

The  $h$ - $H_i^-$ - $H_j^+$  couplings make important contributions not only to the  $t \rightarrow qh$  processes but also to the  $h \rightarrow \ell\ell'$  processes, where the Feynman diagram for  $h \rightarrow \ell\ell'$  is sketched in Fig. 2, and the current upper limits are given in Table III. The effective  $h$ - $\ell$ - $\ell'$  interactions can be written as:

$$\mathcal{L}_{h\ell\ell'} = -\bar{\ell} (C_{\ell\ell'}^R P_R + C_{\ell\ell'}^L P_L) \ell' h. \quad (28)$$

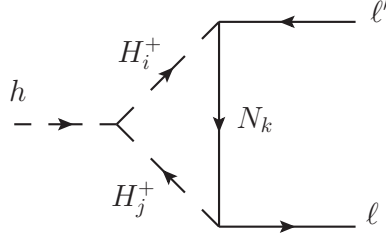


FIG. 2: Feynman diagram for  $h \rightarrow \ell\ell'$  induced by  $H_i^\pm$ .

TABLE III: Experimental upper limits on  $h \rightarrow \ell\ell'$  [94].

Channel	$h \rightarrow e^+e^-$	$h \rightarrow e\mu$	$h \rightarrow e\tau$	$h \rightarrow \mu\tau$
Exp. UL	$3.6 \times 10^{-4}$	$6.1 \times 10^{-5}$	$2.2 \times 10^{-3}$	$1.5 \times 10^{-3}$

Using the Higgs trilinear couplings shown in Eq. (11) and the new Yukawa couplings in Eq. (19), the effective coefficients  $C_{\ell\ell'}^{R,L}$  in the model are obtained as:

$$\begin{aligned}
C_{\ell\ell'}^R &= \frac{1}{(4\pi)^2} \sum_{k=1}^2 \frac{v}{m_{N_k}} \sum_{i,j=1}^2 (C_{N_k L}^i)_{\ell'} \lambda_{ij}^h J_{hk}^{ij} (C_{N_k R}^j)_\ell \\
&= \frac{1}{(4\pi)^2} \sum_{k=1}^2 \frac{v}{m_{N_k}} \left[ \frac{s_{2\theta_\chi}}{2} (\lambda_{22}^h J_{hk}^{22} - \lambda_{11}^h J_{hk}^{11}) - c_{2\theta_\chi} \lambda_{12}^h J_{hk}^{12} \right] (\mathbf{y}_{1k}^\ell)_\ell (\mathbf{y}_{2k}^\ell)_{\ell'}, \\
C_{\ell\ell'}^L &= \frac{1}{(4\pi)^2} \sum_{k=1}^2 \frac{v}{m_{N_k}} \sum_{i,j=1}^2 (C_{N_k R}^i)_{\ell'} \lambda_{ij}^h J_h^{ij} (C_{N_k L}^j)_\ell \\
&= \frac{1}{(4\pi)^2} \sum_{k=1}^2 \frac{v}{m_{N_k}} \left[ \frac{s_{2\theta_\chi}}{2} (\lambda_{22}^h J_{hk}^{22} - \lambda_{11}^h J_{hk}^{11}) - c_{2\theta_\chi} \lambda_{12}^h J_{hk}^{12} \right] (\mathbf{y}_{2k}^\ell)_\ell (\mathbf{y}_{1k}^\ell)_{\ell'}, \quad (29)
\end{aligned}$$



$$J_{hk}^{ij} = \int_0^1 dx_1 \int_0^{x_1} dx_2 \frac{1}{1 - (1 - r_{H_i^\pm}^k)x_1 + (r_{H_j^\pm}^k - r_{H_i^\pm}^k)x_2 + r_h^k x_2(x_2 - x_1)}, \quad (30)$$

with  $r_F^k \equiv m_F^2/m_{N_k}^2$ . It can be seen that  $C_{\ell\ell'}^R = C_{\ell'\ell}^L$ . The branching ratio of the  $h \rightarrow \ell\ell'$  decay is then:

$$BR(h \rightarrow \ell\ell') = \frac{\zeta_{\ell\ell'} m_h}{16\pi\Gamma_h} (|C_{\ell\ell'}^R|^2 + |C_{\ell\ell'}^L|^2), \quad (31)$$

where  $\zeta_{\ell\ell} = 1$  and  $\zeta_{\ell\ell'} = 2$ .

### C. Radiative lepton flavor violation and lepton $g-2$

The radiative LFV processes can be induced via the  $\gamma$ -penguin diagram mediated by the inert charged Higgs boson. Using the Yukawa couplings in Eq. (19) and gauge coupling in Eq. (15), the loop-induced effective  $\ell$ - $\ell'$ - $\gamma$  interactions can be written as:

$$\mathcal{L}_{\ell'\ell\gamma}^\gamma = e \bar{\ell}' i \sigma_{\mu\nu} (C_{R\ell'\ell}^\gamma P_R + C_{L\ell'\ell}^\gamma P_L) \ell \epsilon^{\mu*} k^\nu, \quad (32)$$

where the effective coefficients in the model are given by:

$$\begin{aligned} C_{R\ell'\ell}^\gamma &= \sum_{i,k=1}^2 \frac{(C_{N_k R}^i)_{\ell'} (C_{N_k L}^i)_\ell}{(4\pi)^2 m_{N_k}} J_\gamma^1 \left( \frac{m_{H_i^\pm}^2}{m_{N_k}^2}, 0, 0 \right) \\ &= -\frac{s_{2\theta_\chi}}{2(4\pi)^2} \sum_{k=1}^2 \frac{(\mathbf{y}_{2k}^\ell)_{\ell'} (\mathbf{y}_{1k}^\ell)_\ell}{m_{N_k}} \Delta J_\gamma^{1k}, \\ C_{L\ell'\ell}^\gamma &= \sum_{i,k=1}^2 \frac{(C_{N_k L}^i)_{\ell'} (C_{N_k R}^i)_\ell}{(4\pi)^2 m_{N_k}} J_\gamma^1 \left( \frac{m_{H_i^\pm}^2}{m_{N_k}^2}, 0, 0 \right) \\ &= -\frac{s_{2\theta_\chi}}{2(4\pi)^2} \sum_{k=1}^2 \frac{(\mathbf{y}_{1k}^\ell)_{\ell'} (\mathbf{y}_{2k}^\ell)_\ell}{m_{N_k}} \Delta J_\gamma^{1k}, \end{aligned} \quad (33)$$

with

$$\Delta J_\gamma^{1k} = J_\gamma^1 \left( \frac{m_{H_1^\pm}^2}{m_{N_k}^2}, 0, 0 \right) - J_\gamma^1 \left( \frac{m_{H_2^\pm}^2}{m_{N_k}^2}, 0, 0 \right). \quad (34)$$

Because the Yukawa couplings of charged scalars to fermions involve left-handed and right-handed states, the chirality flip occurring in the propagator of the  $N_k$  fermion line leads to an enhancement factor of  $m_{N_k}$ . Therefore,  $C_{R\ell'\ell}^\gamma$  and  $C_{L\ell'\ell}^\gamma$  are only suppressed by  $1/m_{N_k}$  instead of  $1/m_{N_k}^2$ . Moreover, for the photon radiative decays, although  $m_{H_i^\pm}^2/m_{N_k}^2 \ll 1$ , we cannot take  $\Delta J_\gamma^{1k} \sim 0$  in Eq. (34); otherwise,  $C_{R\ell'\ell}^\gamma \sim C_{L\ell'\ell}^\gamma \sim 0$ . The branching ratio of

$\ell \rightarrow \ell' \gamma$  can be estimated using:

$$BR(\ell \rightarrow \ell' \gamma) \approx \frac{\tau_\ell \alpha m_\ell^3}{4} \left( |C_{R\ell'\ell}^\gamma|^2 + |C_{L\ell'\ell}^\gamma|^2 \right), \quad (35)$$

where  $\tau_\ell$  denotes the lifetime of  $\ell$  lepton.

From the electromagnetic dipole interactions in Eq. (32), the lepton  $g-2$  can be obtained in a straightforward way by taking  $\ell' = \ell$  and given by:

$$\begin{aligned} \Delta a_\ell &= \frac{m_\ell}{8\pi^2} \sum_{i,k=1}^2 \frac{(C_{N_k L}^i)_\ell (C_{N_k R}^i)_\ell}{m_{N_k}} J_\gamma^1 \left( \frac{m_{H_i^\pm}^2}{m_{N_k}^2}, 0, 0 \right) \\ &= -\frac{m_\ell s_{2\theta_\chi}}{16\pi^2} \sum_{k=1}^2 \frac{(\mathbf{y}_{1k}^\ell)_\ell (\mathbf{y}_{2k}^\ell)_\ell}{m_{N_k}} \Delta J_\gamma^1. \end{aligned} \quad (36)$$

In general, the above lepton  $g-2$  correction can be positive or negative, depending on the signs of  $s_{\theta_\chi}$  and  $(\mathbf{y}_{1k(2k)}^\ell)_\ell$ .

#### D. Oblique parameters and $W$ boson mass

In addition to enhancing the rare decays in the SM, the newly introduced particles and couplings can make significant contributions to the vacuum polarization tensors, parametrized by [88]

$$\Pi_{VV'}^{\mu\nu}(q) = g^{\mu\nu} A_{VV'}(q^2) + q^\mu q^\nu B_{VV'}(q^2), \quad (37)$$

where  $VV'$  can be the gauge boson pairs  $\gamma\gamma$ ,  $\gamma Z$ ,  $ZZ$ , and  $WW$ . To show the sensitivity to the new physics effects, we can use the oblique parameters  $S$ ,  $T$ , and  $U$ , which are related to  $A_{VV'}(q^2)$  and defined as [89–91]:

$$\begin{aligned} \alpha T &= \frac{A_{WW}(0)}{m_W^2} - \frac{A_{ZZ}(0)}{m_Z^2}, \\ \frac{\alpha}{4s_W c_W} S &= \frac{A_{ZZ}(m_Z^2) - A_{ZZ}(0)}{m_Z^2} - \frac{\partial A_{\gamma\gamma}(q^2)}{\partial q^2} \Big|_{q^2=0} + \frac{c_W^2 - s_W^2}{s_W c_W} \frac{\partial A_{\gamma Z}(q^2)}{\partial q^2} \Big|_{q^2=0}, \\ U + S &= \frac{4s_W^2}{\alpha} \left( \frac{A_{WW}(m_W^2) - A_{WW}(0)}{m_W^2} - \frac{\partial A_{\gamma\gamma}(q^2)}{\partial q^2} \Big|_{q^2=0} + \frac{c_W}{s_W} \frac{\partial A_{\gamma Z}(q^2)}{\partial q^2} \Big|_{q^2=0} \right). \end{aligned} \quad (38)$$

Since the  $U$  parameter can be taken as the effect of a dimension-8 operator and is normally much smaller than  $T$  and  $S$  that are due to the effects of dimension-6 operators, we take  $U \approx 0$  in the model.

Because the  $Z_2$ -odd  $B$  quark and  $N$  are singlets and do not mix with the SM fermions, they do not contribute to the  $T$  and  $S$  parameters. Thus, only the inert Higgs doublet  $H_I$  and the charged singlet  $\chi^\pm$  will affect the oblique parameters. According to the results obtained in Ref. [92], the  $T$  parameter from  $H_I$  and  $\chi^\pm$  is given by:

$$T = \frac{1}{16\pi^2 c_W^2 s_W^2} \left[ c_{\theta_\chi}^2 \left( \theta_+(z_{H_1^\pm}, z_{H_I}) + \theta_+(z_{H_1^\pm}, z_{A_I}) \right) + s_{\theta_\chi}^2 \left( \theta_+(z_{H_2^\pm}, z_{H_I}) + \theta_+(z_{H_2^\pm}, z_{A_I}) \right) - \frac{1}{2} c_{\theta_\chi}^2 s_{\theta_\chi}^2 \theta_+(z_{H_1^\pm}, z_{H_2^\pm}) - \theta_+(z_{H_I}, z_{A_I}) \right], \quad (39)$$

with  $z_f \equiv m_f^2/m_Z^2$  and

$$\theta_+(x, y) = x + y - \frac{2xy}{x - y} \ln \left( \frac{x}{y} \right). \quad (40)$$

The  $S$  parameter, on the other hand, is:

$$S = \frac{1}{\pi} \left[ G(1, z_{S_I}, z_{A_I}) + c_{\theta_\chi}^2 (1 - s_{\theta_\chi}^2) G(1, z_{H_1^\pm}, z_{H_1^\pm}) - s_{\theta_\chi}^2 (1 + c_{\theta_\chi}^2) G(1, z_{H_2^\pm}, z_{H_2^\pm}) + 2s_{\theta_\chi}^2 c_{\theta_\chi}^2 G(1, z_{H_1^\pm}, z_{H_2^\pm}) \right], \quad (41)$$

where

$$G(a, b, c) = B_{22}(a, b, c) - B_{22}(0, b, c),$$

$$B_{22}(a, b, c) = -\frac{1}{2} \int_0^1 dx (bx + c(1-x) - ax(1-x)) \ln (bx + c(1-x) - ax(1-x)). \quad (42)$$

From the results, it can be seen that when  $\chi^\pm$  decouples from  $H_I^\pm$ , i.e.  $s_{\theta_\chi} = 0$ , only the inert Higgs doublet contributes to the oblique parameters.

It is known that the relation of  $m_W$  to the oblique parameters can be expressed as [91]:

$$m_W = m_W^{\text{SM}} \left[ 1 + \frac{\alpha}{c_W^2 - s_W^2} \left( c_W^2 T - \frac{S}{2} + \frac{c_W^2 - s_W^2}{4s_W^2} U \right) \right]^{1/2}$$

$$\simeq m_W^{\text{SM}} \left[ 1 + \frac{\alpha}{4(c_W^2 - s_W^2)} (2c_W^2 T - S) \right], \quad (43)$$

where we have neglected  $U$  parameter in the linear approximation in the second line as it is much smaller than  $T$  and  $S$ . Taking  $s_W^2 = 0.2316$ ,  $\alpha = 1/129$ , and  $m_W^{\text{SM}} = 80.3496$  [83] as the SM inputs, we find that when  $T \sim 0.16$  and  $S \sim -0.02$ , the  $W$  boson mass can be increased to  $m_W \approx 80.4267$  GeV. In the section of numerical analysis, we will show the correlation of the parameters with the necessary values of  $T$  and  $S$  to explain the  $m_W$  anomaly.

## IV. CONSTRAINTS

We discuss potentially strict constraints on the model in this section. In addition to  $\mu \rightarrow e\gamma$  mentioned earlier, we discuss the severe limits from  $\Delta B = 2$ ,  $\Delta D = 2$ , and  $h \rightarrow \gamma\gamma$  processes. Since the considered mass scale of the inert scalars is set at the EWSB scale, the lightest neutral component, i.e.  $S_I$  or  $A_I$ , can be a DM candidate. In this case, the Higgs trilinear coupling  $h-S_I-S_I$  or  $h-A_I-A_I$  will be constrained by the DM direct detection through Higgs portal. Nevertheless, because the involved coupling is  $\lambda_L$  and it is not directly related to the processes studied in this work, one can take the  $\lambda_L \sim 0$  limit to satisfy the nonobservation of DM direct detection.

### A. $\Delta B = 2$ and $\Delta D = 2$ processes

From Eq. (19), it is seen that the down-type quarks couple to  $Z_2$ -odd  $B$  quark and inert neutral scalars. Thus,  $\Delta B = 2$  processes induced via box diagrams can give stringent constraints on the Yukawa couplings  $\mathbf{y}_2^B$ . To estimate the  $B_{q'} - \bar{B}_{q'}$  mixing parameter, we simply use the hadronic effect  $\langle \bar{B} | (\bar{q}' \gamma_\mu P_L b)^2 | B_{q'} \rangle \sim f_{B_{q'}}^2 m_{B_{q'}} / 3$ . The mass difference between the heavy and light  $B$  mesons can be simplified to be:

$$\Delta m_{B_{q'}} \sim \frac{f_{B_{q'}}^2 m_{B_{q'}}}{48\pi^2 m_B^2} \left( (V_{\text{CKM}}^\dagger \mathbf{y}_2^B)_{q'} (\mathbf{y}_2^{B\dagger} V_{\text{CKM}})_3 \right)^2, \quad (44)$$

where the approximation  $m_{S_I, A_I}^2 / m_B^2 \sim 0$  appearing in the loop integrals is applied. Due to the fact that  $(V_{\text{CKM}})_{k3} \ll 1$  ( $k = 1, 2$ ), we have  $(\mathbf{y}_2^{B\dagger} V_{\text{CKM}})_3 \sim y_{23}^B$ ,

$$\begin{aligned} (V_{\text{CKM}}^\dagger \mathbf{y}_2^B)_d &\sim -\lambda y_{22}^B + y_{21}^B, \\ (V_{\text{CKM}}^\dagger \mathbf{y}_2^B)_s &\sim y_{22}^B + \lambda y_{21}^B, \end{aligned} \quad (45)$$

with  $\lambda \sim 0.22$  being the Wolfenstein parameter. If we assume  $y_{21}^B \sim \lambda y_{22}^B$  to avoid the  $\Delta m_{B_d}$  constraint,  $(V_{\text{CKM}}^\dagger \mathbf{y}_2^B)_s \sim y_{22}^B$  is then bounded by  $\Delta m_{B_s}$ . Taking  $f_{B_s} = 0.231$  GeV [93] and requiring  $\Delta m_{B_s} < \Delta m_{B_s}^{\text{exp}} = 1.17 \times 10^{-11}$  GeV [94], the upper limit on  $f_{22}^B f_{23}^B$  can be obtained as:

$$\frac{|f_{22}^B f_{23}^B|}{m_B} < 1.4 \times 10^{-4}. \quad (46)$$

If we just consider the contributions from  $f_{22,23}^B$  and ignore the other parameters, the branching ratios of top-FCNCs will be smaller than  $10^{-6}$  and lower than the sensitivities of HL-LHC.

Hence, if  $f_{21}^B$  and  $f_{22}^B$  are bounded by  $\Delta m_{B_d}$  and  $\Delta m_{B_s}$ , respectively, their effects can be neglected.

From Eq. (19), it can be found that the couplings to the  $Z_2$ -odd  $B$  quark and inert charged scalars only involve the left-handed up-type quarks. As a result,  $f_{11}^B$  and  $f_{12}^B$  contribute to the  $D$ - $\bar{D}$  mixing, and the resulting mixing parameter of  $D$  meson can be written as:

$$\Delta m_D \sim -\frac{f_D^2 m_D}{12(4\pi)^2 m_B^2} (y_{11}^B y_{12}^B)^2, \quad (47)$$

where we have applied the approximation  $m_{H_i^\pm}^2/m_B^2 \sim 0$ . With  $f_D = 0.213$  GeV [94] and  $\Delta m_D^{\text{exp}} = 6.1 \times 10^{-15}$  GeV, the upper limit on  $f_{11}^B f_{12}^B$  is

$$\frac{|f_{11}^B f_{12}^B|}{m_B} < 1.2 \times 10^{-5}. \quad (48)$$

Combing the constraints shown in Eqs. (46) and (48), we conclude that  $t \rightarrow u(h, V)$  and  $t \rightarrow c(h, V)$  cannot be simultaneously enhanced up to the sensitivities of HL-LHC. Thus, in the following analysis, we assume  $f_{11}^B \ll f_{12,13}^B$  and  $f_{21,22}^B \ll f_{23}^B$  and focus on the  $t \rightarrow c$  FCNC processes.

## B. $h \rightarrow \gamma\gamma$

As stated earlier, the Higgs trilinear couplings to  $H_i^\pm$  make significant contributions to  $t \rightarrow qh$  and  $h \rightarrow \ell\ell'$ ; it is found that the same couplings can also modify the Higgs to diphoton decay rate. Since the measurement of  $h \rightarrow \gamma\gamma$  is approaching a precision level, it is expected that the associated free parameters may suffer from a strict bound. To study the new physics effects on  $h \rightarrow \gamma\gamma$ , let's consider the signal strength of  $pp \rightarrow h \rightarrow \gamma\gamma$  defined by:

$$\mu_{\gamma\gamma} = \frac{\sigma(pp \rightarrow h)}{\sigma(pp \rightarrow h)^{\text{SM}}} \frac{BR(h \rightarrow \gamma\gamma)}{BR(h \rightarrow \gamma\gamma)^{\text{SM}}}, \quad (49)$$

where the current world average is  $\mu_{\gamma\gamma} = 1.10 \pm 0.07$  [94].

The loop-induced effective interaction for  $h\gamma\gamma$  can be parameterized as:

$$\mathcal{L}_{hVV} = \frac{\alpha}{4\pi} \frac{a_{\gamma\gamma}}{m_h} h F_{\mu\nu} F^{\mu\nu}, \quad (50)$$

where the Feynman diagrams mediated by  $H_i^\pm$  are shown in Fig. 3. The resulting  $a_{\gamma\gamma}$  in the model is obtained as:

$$a_{\gamma\gamma} = \frac{gm_h}{2m_W} \left( a_{2\gamma}^{\text{SM}} + \sum_{i=1}^2 \frac{\lambda_i^h v m_W}{gm_{H_i^\pm}^2} F_0(\tau_{H_i^\pm}) \right), \quad (51)$$

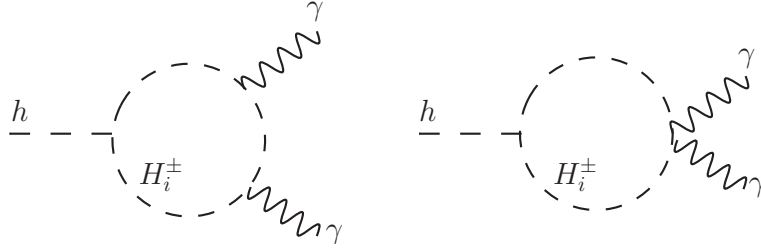


FIG. 3: Feynman diagrams for  $h \rightarrow \gamma\gamma$  induced by  $H_I^\pm$ .

where  $a_{2\gamma}^{\text{SM}} \approx 6.51 - i0.02$  is the SM, and the function  $F_0$  is

$$F_0(\tau) = \tau(1 - \tau f(\tau)), \quad (52)$$

with  $\tau \equiv 4m_f^2/m_{H_i^\pm}^2$  and  $f(\tau) = (\arcsin(1/\sqrt{\tau}))^2$ .

Because the SM Higgs does not couple to the  $B$  quark, the signal strength for  $pp \rightarrow h \rightarrow \gamma\gamma$  can be simplified as

$$\mu_{\gamma\gamma} \approx \frac{BR(h \rightarrow \gamma\gamma)}{BR(h \rightarrow \gamma\gamma)^{\text{SM}}} \approx \left| 1 + \sum_{i=1}^2 \frac{\lambda_{ii}^h v m_W}{g m_{H_i^\pm}^2 a_{2\gamma}^{\text{SM}}} F_0(\tau_{H_i^\pm}) \right|^2, \quad (53)$$

where the new physics contribution to the Higgs width  $\Gamma_h$  is assumed to be small and neglected in the calculation of  $\mu_{\gamma\gamma}$ . To suppress the invisible Higgs decay  $h \rightarrow S_I S_I, A_I A_I$  and to have  $\Gamma_h \approx \Gamma_h^{\text{SM}} \approx 4.1$  MeV, we simply take  $m_h < 2m_{S_I, A_I}$  in the model. Using  $m_{H_{1,2}^\pm} = (120, 320)$  GeV, the  $H_i^\pm$  effect on  $\mu_{\gamma\gamma}$  can be estimated to be  $-0.125\lambda_{11}^h - 0.015\lambda_{22}^h$ . Because  $\mu_{\gamma\gamma}$  arising from  $H_i^\pm$  is proportional to  $1/m_{H_i^\pm}^2$ , it is seen that the influence of heavy  $H_2^\pm$  is small. If we take the allowed range of  $\mu_{\gamma\gamma}$  to be  $0.9 < \mu_{\gamma\gamma} < 1.2$  and drop the  $H_2^\pm$  contribution, then  $\lambda_{11}^h$  can be restricted to fall in the range  $-0.8 < \lambda_{11}^h < 0.5$ . Hence, the  $\lambda_{11}^h$  parameter can be bounded by the  $h \rightarrow \gamma\gamma$  measurement, whereas the region of  $\lambda_{22}^h$  is wide.

### C. $\mu \rightarrow e\gamma$ decay

The current experimental upper limits on  $\ell \rightarrow \ell'\gamma$  are listed in Table IV [94]. It can be seen that the constraint from  $\mu \rightarrow e\gamma$  should be much stronger than that from the  $\tau$  decays.

In order to satisfy the upper limit of  $\mu \rightarrow e\gamma$ , we assume that the free parameters can satisfy the conditions  $C_{Re\mu}^\gamma \approx 0$  and  $C_{Le\mu}^\gamma \approx 0$ , where  $C_{R\ell'\ell}^\gamma$  and  $C_{L\ell'\ell}^\gamma$  are defined in Eq. (33).

TABLE IV: Experimental upper limits on  $\ell \rightarrow \ell' \gamma$  decays [94].

Channel	$\mu \rightarrow e \gamma$	$\tau \rightarrow e \gamma$	$\tau \rightarrow \mu \gamma$
Exp. UL	$4.2 \times 10^{-13}$	$3.3 \times 10^{-8}$	$4.2 \times 10^{-8}$

As a result, the relevant Yukawa couplings can be related as:

$$\begin{aligned}
(y_{22}^\ell)_e &\approx -\frac{m_{N_2}}{m_{N_1}} \frac{\Delta J_\gamma^{11}}{\Delta J_\gamma^{12}} \frac{(y_{11}^\ell)_\mu}{(y_{12}^\ell)_\mu}, \\
(y_{12}^\ell)_e &\approx -\frac{m_{N_2}}{m_{N_1}} \frac{\Delta J_\gamma^{11}}{\Delta J_\gamma^{12}} \frac{(y_{21}^\ell)_\mu}{(y_{22}^\ell)_\mu}.
\end{aligned} \tag{54}$$

If we further take  $m_{N_1} = m_{N_2}$ , in addition to  $BR(\mu \rightarrow e \gamma) \approx 0$ , we will also have  $BR(h \rightarrow e \mu) \approx 0$ .

## V. NUMERICAL ANALYSIS

### A. Parameter setting

The relevant free parameters introduced in the model are the Yukawa couplings  $\mathbf{y}_{1,2}^B$  and  $\mathbf{y}_{1k,2k}^\ell$ , the mixing angle  $\theta_\chi$ , the masses of inert scalars  $m_{H_i^\pm, S_I, A_I}$ , the masses of new fermions  $m_{B_i, N_k}$ , and the scalar couplings from the scalar potential  $\lambda_{ij}^h$  defined in Eq. (11). Although some constraints on the free parameters have been studied earlier, in the following we make some more considerations to further restrict their ranges before scanning the observables.

Generally, each of  $N$  and  $S_I(A_I)$  can be a DM candidate. Since we concentrate on the scenario where  $m_{S_I(A_I)} \sim \mathcal{O}(m_W)$ , as it can fit the observed DM relic density [80], we take  $m_N > m_{S_I(A_I)}$  in this work. To be specific, we assume  $m_{S_I} < m_{A_I, H_i^\pm}$  so that  $S_I$  is the DM candidate. Because the oblique parameters are sensitive to the mass differences among  $H_i^\pm$ ,  $S_I$ , and  $A_I$ , we first discuss the constraint from the  $T$  and  $S$  parameters. Using Eqs. (39) and (41), we make the scatter plot for the correlation between  $m_{H_1^\pm} - m_{S_I}$  and  $m_{A_I} - m_{S_I}$  in Fig. 4(a), where we take  $s_{\theta_\chi} \in (-1/\sqrt{2}, 1/\sqrt{2})$ ,  $m_{S_I, A_I, H_1^\pm} \in (70, 300)$  GeV,  $m_{H_2^\pm} \in (70, 500)$  GeV, and  $T = 0.202 \pm 0.056$  and  $S = 0.100 \pm 0.073$  [83] with  $2\sigma$  errors as the allowed ranges. For the purpose of comparison, we show the result with  $s_{\theta_\chi} = 0$  in Fig. 4(b). It can be seen that to fit the results of  $T$  and  $S$ , the allowed range of  $m_{H_1^\pm} - m_{S_I}$

with  $s_{\theta_\chi} \neq 0$  is broader than that with vanishing  $s_{\theta_\chi}$ . The correlation between  $m_{H_2^\pm} - m_{H_1^\pm}$  and  $m_{H_1^\pm} - m_{A_I}$  is shown in Fig. 4(c). The dependence of  $m_W$  on  $S$  and  $T$  in the model is exhibited in Fig. 4(d). From the results, we see that the  $W$ -mass anomaly can be explained if  $-0.05 < S < 0.02$  and  $0.10 < T < 0.26$ .

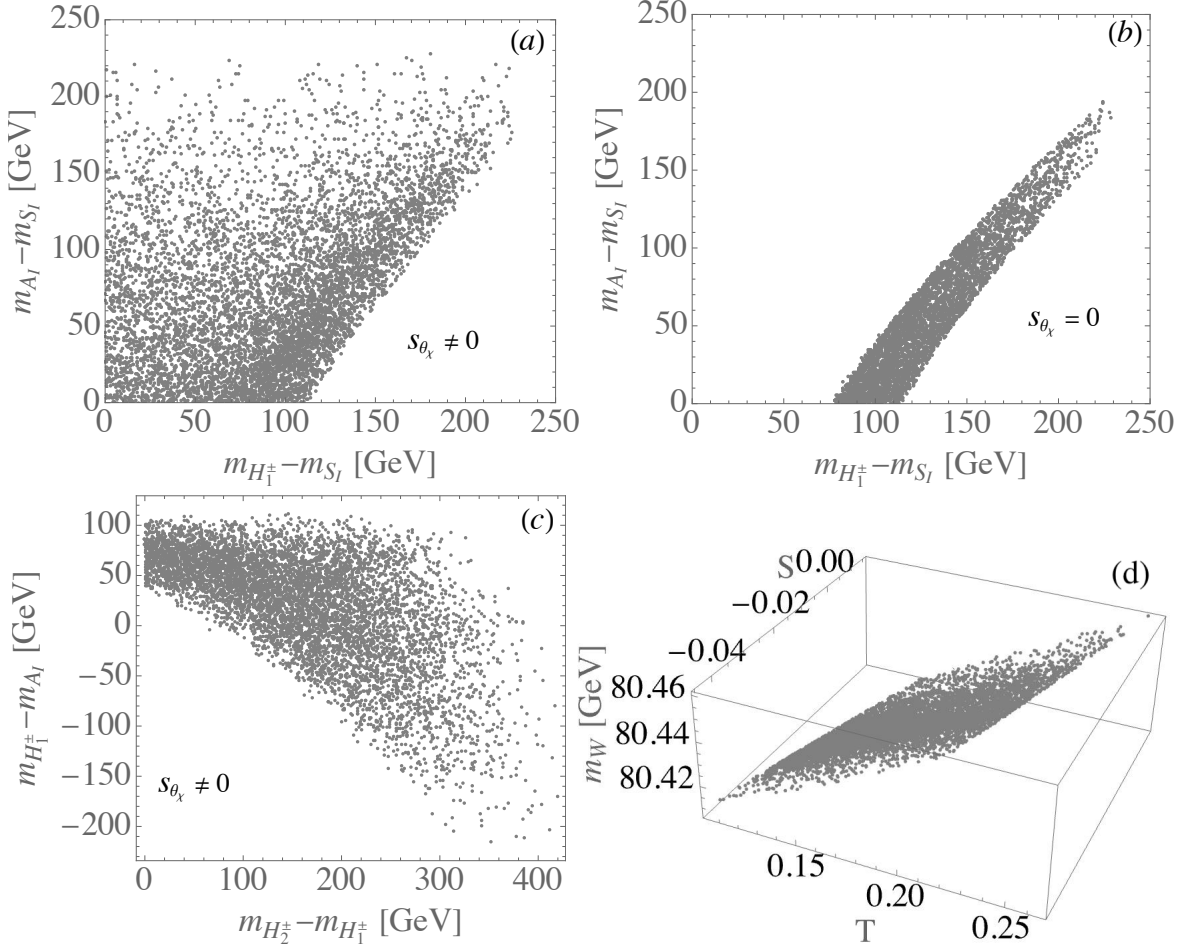


FIG. 4: Correlation between  $m_{H_1^\pm} - m_{S_I}$  and  $m_{A_I} - m_{S_I}$  for (a)  $s_{\theta_\chi} = 0$  and (b)  $s_{\theta_\chi} \neq 0$ ; (c) correlation between  $m_{H_2^\pm} - m_{H_1^\pm}$  and  $m_{H_1^\pm} - m_{A_I}$ , and (d) the resulting  $m_W$  as a function of  $T$  and  $S$  parameters, where  $T = 0.202 \pm 0.056$  and  $S = 0.100 \pm 0.073$  in their  $2\sigma$  ranges.

In addition to the constraints from  $\Delta B = 2$  and  $\Delta D = 2$ , we can also use the perturbative unitarity constraint to bound the Yukawa couplings, where the upper limits are required to be  $|\mathbf{y}_{1,2}^B|, |\mathbf{y}_{1k,2k}^\ell| < \sqrt{4\pi}$  [95]. For the mass upper limit of the  $Z_2$ -odd quark, we can apply the constraints on the stop and sbottom with the  $R$ -parity conserving supersymmetry (SUSY). Using the data with an integrated luminosity of  $139 \text{ fb}^{-1}$  at  $\sqrt{s} = 13 \text{ TeV}$  [96], the mass



below 1 TeV has been excluded by ATLAS when the neutralino mass is around 100 GeV. Therefore, we impose  $m_B > 1$  TeV. Although there is no strict limit on the neutral singlet lepton, we take  $m_N > 1$  TeV in the numerical analysis.

To simplify the parameter scan, the ranges of parameters satisfying the theoretical requirements and the experimental bounds are chosen as follows:

$$y_{12,13,23}^B \in (-3.5, 3.5), \mathbf{y}_{1k,2k}^\ell \in (-0.5, 0.5), \lambda_3 \in (1, 5), s_{\theta_\chi} \in \left(-\frac{1}{\sqrt{2}}, \frac{1}{\sqrt{2}}\right),$$

$$m_B \in (1, 1.5) \text{ TeV}, m_{N_1} \in (1, 2) \text{ TeV}, m_{N_2} = m_{N_1} + 300 \text{ GeV}, \quad (55)$$

where we take  $y_{11,21,22}^B \approx 0$  in order not to upset the  $B_{q'} - \bar{B}_{q'}$  and  $D - \bar{D}$  mixing phenomena, as discussed before. To satisfy the constraint from  $h \rightarrow \gamma\gamma$ , we set  $\lambda_{11}^h \approx 0$ . As a result, we have:

$$\lambda_2^\chi = s_{\theta_\chi} c_{\theta_\chi} \left( \frac{m_{H_2^\pm}^2 - m_{H_1^\pm}^2}{v^2} - \lambda_3 \frac{c_{\theta_\chi}^2}{s_{\theta_\chi}^2} \right). \quad (56)$$

Thus, in the numerical calculations, we use Eq. (56) and require  $|\lambda_2^\chi| < 5$ . Moreover, because  $m_{B,N} \gg m_{H_{1,2}^\pm}$ , the phenomenological results will not be sensitivity to the values of  $m_{H_{1,2}^\pm}$ . In the numerical analysis, we fix  $m_{H_1^\pm} = 120$  GeV and  $m_{H_2^\pm} = 320$  GeV, which satisfy the constraints from the  $T$  and  $S$  parameters. In addition, the direct search bounds from colliders on  $m_{H_{I,A_I}}$  are not very strict, and the bound on  $m_{H_I^\pm}$ , reinterpreted from the SUSY search at LEP, is  $m_{H_I^\pm} > 70 - 90$  GeV [97–100].

As alluded to before, the current upper bounds on the BRs of  $t \rightarrow c(h, Z)$  and  $h \rightarrow \mu\tau$  are less than  $10^{-3}$ ,  $5 \times 10^{-4}$ , and  $1.5 \times 10^{-3}$ , respectively. In order to study the model predictions for these modes while avoiding the parameter space that is beyond the HL-LHC sensitivities, we further set low bounds on them when scanning the viable parameters. The ranges of the physical processes used to confine our parameter scan are summarized as follows:

$$BR(t \rightarrow ch) \in (10^{-5}, 10^{-3}), BR(t \rightarrow cZ) \in (0.2, 5) \times 10^{-4}, BR(h \rightarrow ee) < 3.6 \times 10^{-4},$$

$$BR(h \rightarrow e\mu) < 6.1 \times 10^{-5}, BR(h \rightarrow \mu\tau) > 0.5 \times 10^{-4}, BR(\tau \rightarrow e\gamma) < 3.3 \times 10^{-8},$$

$$BR(\tau \rightarrow \mu\gamma) < 4.2 \times 10^{-8}, a_\mu \in (1, 5) \times 10^{-9}, a_e \in (-13, 8) \times 10^{-13}. \quad (57)$$

Since the resulting  $BR(h \rightarrow \mu\tau)$  is much smaller than the current upper limit, we only use the low bound to constrain the parameters. We note that the ranges of  $a_\mu$  and  $a_e$  are taken in such a way that  $a_\mu$  can be positive and around  $O(10^{-9})$ , and the obtained values of  $a_e$  are sufficiently wide so that the current experimental results shown in Eq. (2) can be covered.

## B. Numerical analysis and discussions

In this subsection, we discuss the numerical results for the BRs of  $t \rightarrow c(h, \gamma, Z)$ ,  $\tau \rightarrow (e, \mu)\gamma$ ,  $h \rightarrow \ell\ell'$ , and lepton  $g - 2$  when the parameter ranges given in Eqs. (55) and (57) are used. We first note that because of the constraint of  $D$ -meson mixing, FCNCs for  $t \rightarrow c$  and  $t \rightarrow u$  processes cannot be simultaneously enhanced up to the sensitivities of HL-LHC. We focus on the  $t \rightarrow c$  processes in the following analysis. Although the BR of  $h \rightarrow \tau^-\tau^+$  in the SM is at the percent level, we here only exhibit the purely new physics effects in the numerical analysis.

### 1. Top-FCNCs

To see the distributions of parameters that fit the ranges of  $t \rightarrow c(h, Z)$  given in Eq. (57), we show the scatter plots for the correlations of parameters in Fig. 5, where plots (a), (b), and (c) denote are for the  $y_{13}^B - y_{12}^B$ ,  $y_{13}^B - y_{23}^B$ , and  $\lambda_3 - \lambda_2^x$  planes, respectively. It can be found that to reach the BRs of top-FCNCs at the level of  $\mathcal{O}(10^{-5})$ , the Yukawa couplings  $y_{12,13}^B$  have to be large and are restricted in a narrow range of  $|y_{12,13}^B| \lesssim (2.6, 3.5)$ , whereas  $y_{23}^B$  is wider and  $|y_{23}^B| \lesssim (0.3, 3.5)$ . From Eqs. (25) and (26), it is known that  $BR(t \rightarrow ch/cZ)$  do not vanish when  $s_{\theta_x} = 0$ . However, because we require that all parameters have to fit the chosen ranges in Eq. (57) for the top decays, the values of  $s_{\theta_x}$  may influence their BRs. Thus, we show the correlation between  $s_{\theta_x}$  and  $\lambda_3$  in Fig. 5(d).

After obtaining the available parameter space, we show the BRs of the top-FCNC decays as a function of different parameters in Fig. 6. Since  $y_{12,13}^B$  are constrained within a narrow range, we only exhibit the  $y_{23}^B$  dependence for the Yukawa couplings. From Fig. 6(a), it is seen that  $BR(t \rightarrow ch) \sim \mathcal{O}(10^{-4})$  and  $BR(t \rightarrow cZ) \sim \mathcal{O}(10^{-5})$  can be achieved, with the former be possibly more than one order of magnitude larger than the latter. The results can be understood as follows. From Eqs. (25) and (26), the main different factors in  $t \rightarrow ch$  and  $t \rightarrow cZ$  can be expressed as  $[\lambda_{12}^h(c_{\theta_x}^2 - s_{\theta_x}^2) - \lambda_{22}^h s_{\theta_x} c_{\theta_x}]v/m_B$  and  $gs_W^2 Q_B/c_W \sim 0.01$ , respectively. Thus, even with  $c_{\theta_x} \sim s_{\theta_x}$  or  $s_{\theta_x} \sim 0$ , the result  $BR(t \rightarrow ch) \gg BR(t \rightarrow cZ)$  is expected when  $\lambda_{22}^h \sim \mathcal{O}(1)$  or  $\lambda_{12}^h \sim \mathcal{O}(1)$ . In addition, since we have taken  $f_{21,22}^B \approx 0$  due to the constraints of  $\Delta B = 2$  and  $\Delta D = 2$  processes, it is seen that  $t \rightarrow cZ$  becomes independent of  $y_{23}^B$ . Although  $t \rightarrow cZ$  is not sensitive to  $y_{23}^B$ , the excluded region for  $|y_{23}^B| \lesssim$

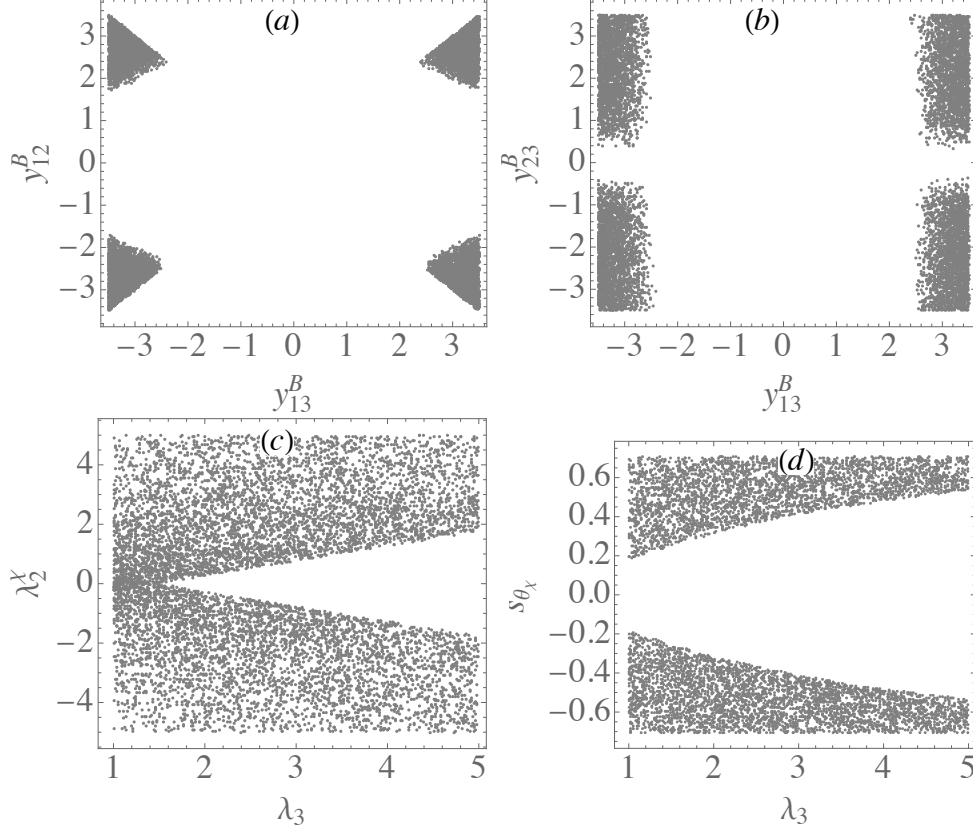


FIG. 5: Scatter plots for the allowed parameter space projected in the planes of: (a)  $y_{13}^B - y_{12}^B$ , (b)  $y_{13}^B - y_{23}^B$ , (c)  $\lambda_3 - \lambda_2^X$ , and (d)  $\lambda_3 - s_{\theta_\chi}$ .

0.4 shown in Fig. 6(a) is from the requirement that the relevant parameters have to satisfy the taken ranges of the top decays shown in Eq. (57).

From Fig. 6(b), we see that the BR for the  $t \rightarrow c\gamma$  decay in the model is far below  $10^{-6}$ . According to Eq. (24), as alluded to earlier, a suppression effect arises from the cancellation between  $H_1^\pm$  and  $H_2^\pm$ . If we take  $m_{H_i^\pm}^2/m_B^2 \approx 0$  in the loop integrals  $J_\gamma^{1,2}$ , the dominant  $B_L^\gamma$  vanishes. We note that  $B_R^\gamma \approx 0$  because  $y_{21,22}^B \approx 0$  is applied. Therefore, using the assumed values of  $m_{H_i^\pm}$ ,  $B_L^\gamma$  is suppressed even though it does not completely vanish. Hence,  $BR(t \rightarrow c\gamma)$  cannot be possibly enhanced up to  $\mathcal{O}(10^{-6})$ . In addition, according to Eq. (21), we see that the BR for  $t \rightarrow cg$  can reach  $\mathcal{O}(10^{-6})$ , which is still much smaller than the upper limit measured by ATLAS with  $BR^{\text{exp}}(t \rightarrow cg) < 3.7 \times 10^{-4}$  [101].

It is known that in addition to the Yukawa couplings, the Higgs trilinear couplings to the charged Higgses  $\lambda_{ij}^h$  defined in Eq. (11) play an important role in the  $t \rightarrow ch$  decay. Since

$\lambda_{ij}^h$  consist of  $\lambda_3$ ,  $\lambda_2^\chi$ , and  $s_{\theta_\chi}$ , to see the dependence of quartic scalar couplings in the decay, the correlation between  $BR(t \rightarrow ch/cZ)$  and  $\lambda_2^\chi$ , defined in Eq. (56), is shown in Fig. 6(c). The resulting dependence pattern for  $\lambda_3$  is similar. Since  $t \rightarrow cZ$  is not related to  $\lambda_3$  and  $\lambda_2^\chi$ , it is seen that  $BR(t \rightarrow cZ)$  is insensitive to the quartic scalar couplings. The dependence of  $BR(t \rightarrow ch/cZ)$  on  $s_{\theta_\chi}$  is shown in Fig. 6(d). As stated earlier, the dominant effects in  $t \rightarrow ch$  are associated with  $c_{\theta_\chi}^2 - s_{\theta_\chi}^2$  and  $s_{\theta_\chi} c_{\theta_\chi}$ , whereas  $t \rightarrow cZ$  is not sensitive to  $s_{\theta_\chi}$  because the decay amplitude results in  $c_{\theta_\chi}^2 + s_{\theta_\chi}^2 = 1$ . Since the parameters need to fit the values given in Eq. (57), we thus obtain a null result of  $t \rightarrow cZ$  in the excluded region of  $|s_{\theta_\chi}| \lesssim 0.2$ .

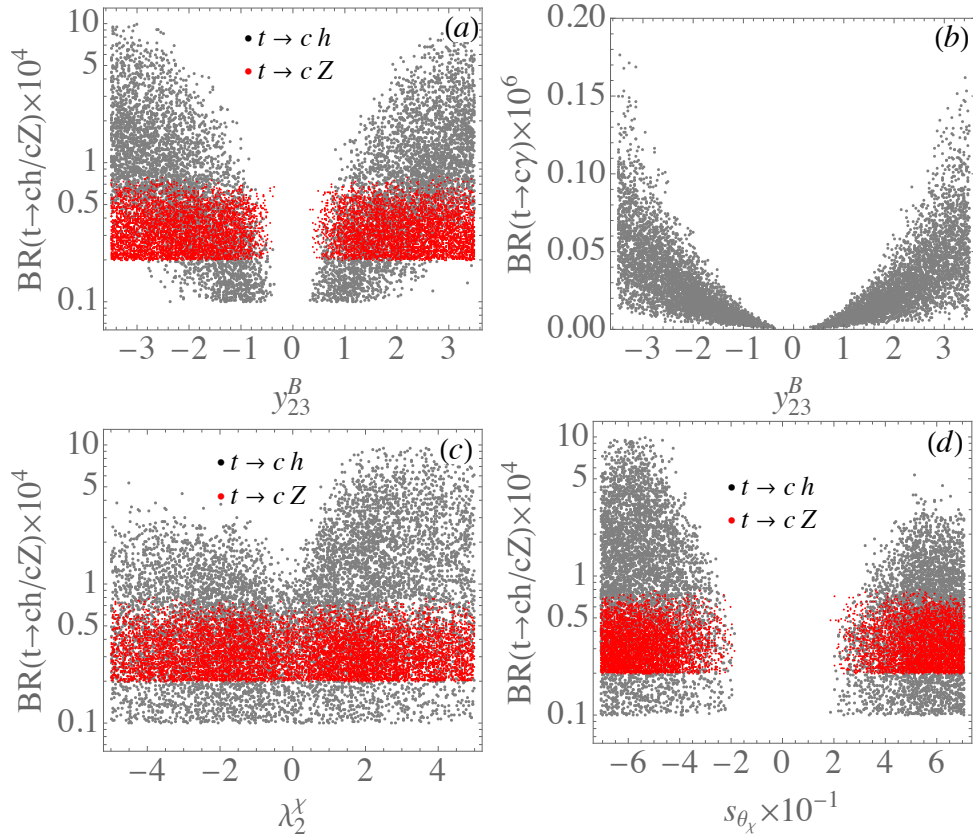


FIG. 6: Scatter plots for  $BR(t \rightarrow ch/cZ)$  as a function of (a)  $y_{23}^B$ , (c)  $\lambda_2^\chi$ , and (d)  $s_{\theta_\chi}$ . Plot (b) is a scatter plot for the correlation between  $BR(t \rightarrow c\gamma)$  and  $y_{23}^B$ .

## 2. Leptonic Higgs decays, radiative LFVs, and lepton $g - 2$

In addition to the Higgs trilinear couplings  $\lambda_{ij}^h$ , the processes  $h \rightarrow \ell_i \ell_j$  as well as  $\ell \rightarrow \ell' \gamma$  and lepton  $g - 2$  are sensitive to the Yukawa couplings  $\mathbf{y}_{1k,2k}^\ell$  and  $m_{N_k}$ . To see the distribution patterns of  $\mathbf{y}_{1k,2k}^\ell$  when the constraints in Eq. (57) are satisfied, we show various correlations of the Yukawa couplings in Fig. 7. Since the correlations among  $\mathbf{y}_{2k}^\ell$  are similar to those among  $\mathbf{y}_{1k}^\ell$ , we only exhibit the scatter plots for the correlations of Yukawa couplings,  $y_{11e}^\ell - y_{11\mu}^\ell$ ,  $y_{11e}^\ell - y_{11\tau}^\ell$ ,  $y_{12e}^\ell - y_{12\mu}^\ell$ , and  $y_{12e}^\ell - y_{12\tau}^\ell$ , in Figs. 7(a)-(d), respectively. From the plots, it can be seen that  $|y_{11e,12e}^\ell|$  have denser sample points below 0.1, whereas the allowed values of  $y_{11\mu,12\mu}^\ell$  and  $y_{11\mu,12\tau}^\ell$  are wider. It is found that the correlations of  $\lambda_3 - \lambda_2^\chi$  and  $\lambda_3 - s_{\theta_\chi}$  in leptonic decays are close to the results shown in Figs. 5(c) and (d); therefore, we skip the related plots.

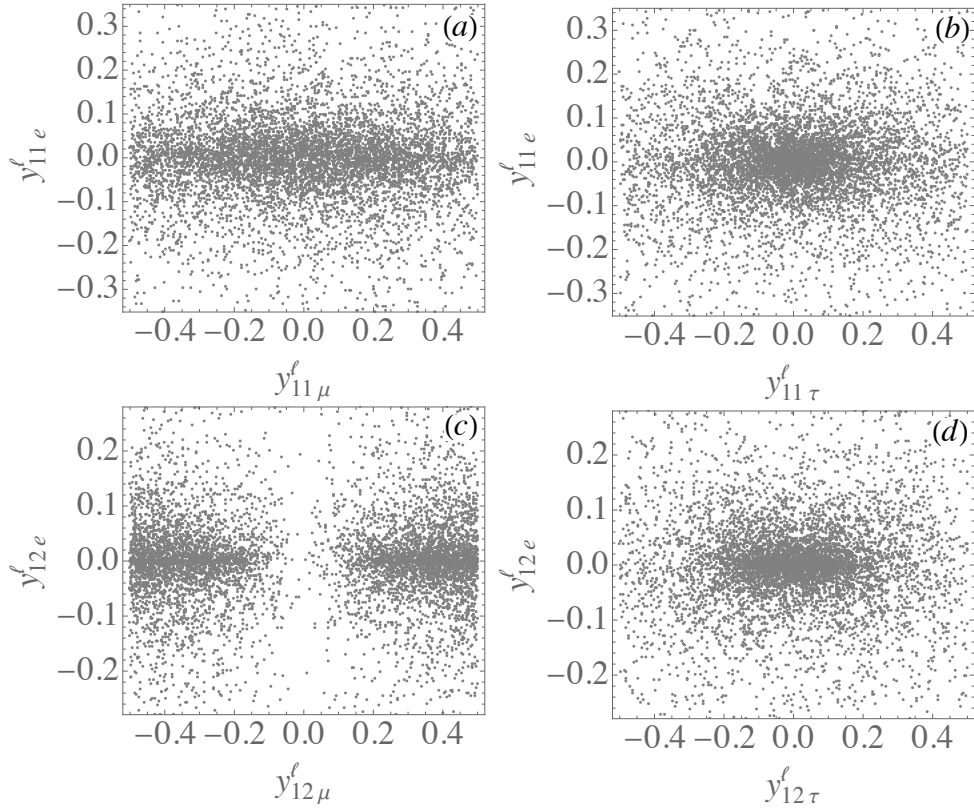


FIG. 7: Scatter plots for the correlations among  $\mathbf{y}_{11}^\ell$  and  $\mathbf{y}_{12}^\ell$ , where the values of parameters are selected to fit the regions of physical observables in Eq. (57).

To see how  $BR(\tau \rightarrow \ell' \gamma)$  are sensitive to the Yukawa couplings, we show the represen-

tative dependence of  $y_{22\tau}^\ell y_{12e}^\ell$  and  $y_{22\tau}^\ell y_{12\mu}^\ell$  for  $\tau \rightarrow e\gamma$  and  $\tau \rightarrow \mu\gamma$  in Figs. 8(a) and (b), respectively, where the product of Yukawa couplings is taken from  $C_{L\ell\ell}^\gamma$  in Eq. (33) and other possible products of Yukawa couplings, such as  $y_{21\tau}^\ell y_{11e}^\ell$  and  $y_{21\tau}^\ell y_{11\mu}^\ell$ , give a similar pattern for each radiative  $\tau$  decay. According to the results in Fig. 7(c), most sampling points for  $|y_{12e}^\ell|$  are located at the values less than 0.1, whereas the distribution of  $|y_{12\mu}^\ell|$  is wider and the sampling points at around 0.1 are suppressed. Hence, the differences of patterns in Figs. 8(a) and (b) can be understood using the results shown in Fig. 7. The correlations with  $s_{\theta_\chi}$  are shown in Fig. 8(c), and the resulting pattern is similar to the  $t \rightarrow ch/cZ$  decays in Fig. 6, where  $|s_{\theta_\chi}| \lesssim 0.2$  cannot fit the assumed ranges in Eq. (57). For the purpose of clarity, we show the correlation plot of  $BR(\tau \rightarrow e\gamma)$  and  $BR(\tau \rightarrow \mu\gamma)$  in Fig. 8(d), where the dashed lines denote the expected sensitivities of Belle II. Since we use the current experimental upper limits to bound the free parameters, most sampling points are located around the regions close to the current upper limits. The sampling points will predict lower  $BR(\tau \rightarrow \ell'\gamma)$  when stricter bounds from experiments are obtained.

Using Eq. (36) and the bounded parameter values obtained in radiative  $\tau$ -lepton decays, we can estimate the contributions to the lepton  $(g-2)$ 's. The correlation between  $\Delta a_e$  and  $\Delta a_\mu$  is shown in Fig. 9, where the band denotes  $\Delta a_\mu^{\text{exp}}$  in its  $2\sigma$  range. It is clearly seen that  $\Delta a_\mu$  in the model can explain the muon  $g-2$  anomaly, and the electron  $g-2$  from the inert charged Higgses has the freedom to be either positive or negative [76]. It is expected that with more precise measurement on the fine structure constant, e.g., from  $\Delta a_e$ , the relevant parameters can be further limited. Since the Yukawa couplings involved in  $\Delta a_e$  and  $\Delta a_\mu$  are different, even the future data exhibit that  $\Delta a_e$  is consistent with the SM prediction,  $\Delta a_\mu \sim \mathcal{O}(10^{-9})$  can still be accommodated by the model.

Next, we discuss the leptonic Higgs decays. From Table III, it is known that the currently strictest upper bounds on the  $h \rightarrow \ell\ell'$  decays are the  $h \rightarrow ee/e\mu$  decays. Combining with the constraints from the charged-lepton decays, the resulting  $BR(h \rightarrow ee)$  and  $BR(h \rightarrow e\mu)$  are shown in Fig. 10(a). It is seen that the BRs of both decays fall preferably at around  $\mathcal{O}(10^{-6})$  though the values of  $\mathcal{O}(10^{-5})$  can be achieved as well. From Fig. 10(b), it can be found that the allowed  $BR(h \rightarrow \mu^+\mu^-)$  is somewhat larger than  $BR(h \rightarrow \tau^+\tau^-)$  and both decays, purely arising from new physics effects, can reach the level of  $\mathcal{O}(10^{-3})$ , with the SM predictions being at  $2.18 \times 10^{-4}$  and  $6.27 \times 10^{-2}$ , respectively [102]. When the SM contributions are included, the  $\mu^+\mu^-$  mode from the new effects is dominant while  $\tau^+\tau^-$

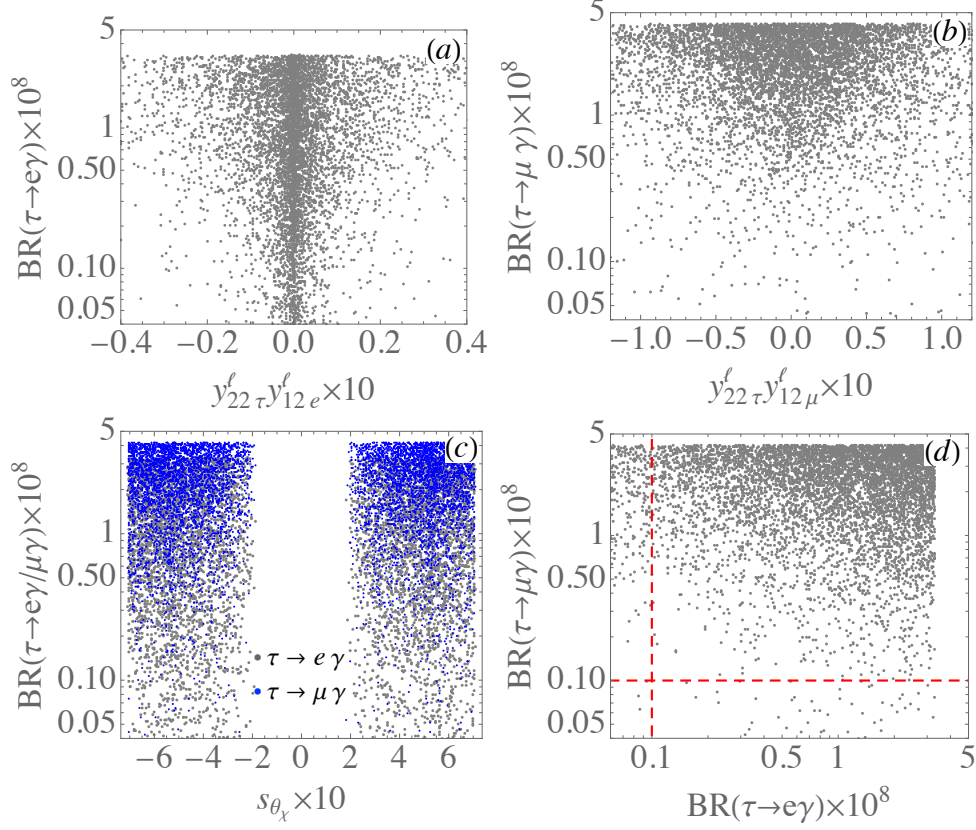


FIG. 8: Scatter plots for  $BR(\tau \rightarrow \ell' \gamma)$  as a function of (a)  $y_{22\tau}^\ell y_{12e}^\ell$  ( $\ell' = e$ ), (b)  $y_{22\tau}^\ell y_{12\mu}^\ell$  ( $\ell = \mu$ ), and (c)  $s_{\theta_\chi}$ . Plot (d) shows the correlation between  $BR(\tau \rightarrow e \gamma)$  and  $BR(\tau \rightarrow \mu \gamma)$ , where the dashed lines are the sensitivity levels of Belle II.

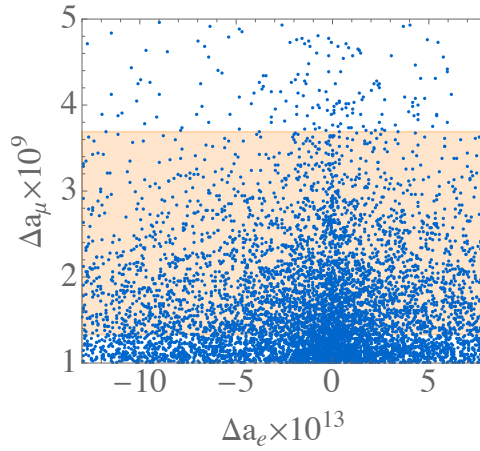


FIG. 9: Correlation between electron and muon  $(g-2)$ 's in the model, where the light orange band denotes the data within  $2\sigma$  errors taken from Eq. (1).

can be maximally changed by 30%. The reason that  $h \rightarrow \tau^+ \tau^-$  has a smaller BR is because the Yukawa couplings  $y_{1k\tau}^\ell$  and  $y_{2k\tau}^\ell$  obtain a stricter constraint from the  $\tau \rightarrow \mu\gamma$  decay, whereas the Yukawa couplings  $y_{2k\mu}^\ell y_{1k\mu}^\ell$  are only bounded by  $\Delta a_\mu \in (1, 5) \times 10^{-9}$ . The BRs for  $h \rightarrow e\tau$  and  $h \rightarrow \mu\tau$  as a correlation to  $BR(h \rightarrow \mu^+ \mu^-)$  are shown in Fig. 10(c) and (d), respectively. The resulting  $BR(h \rightarrow \mu\tau)$  can reach  $\mathcal{O}(10^{-4})$  while  $BR(h \rightarrow e\tau)$  can be of  $\mathcal{O}(10^{-5})$  in the model. From the results in Fig. 7, it can be seen that  $|y_{1k\mu, 2k\mu}^\ell|$  have wide allowed-regions and a little bit larger values; therefore, it can be expected that the resulting  $BR(h \rightarrow \mu\tau)$  can be larger than  $BR(h \rightarrow e\tau)$ .

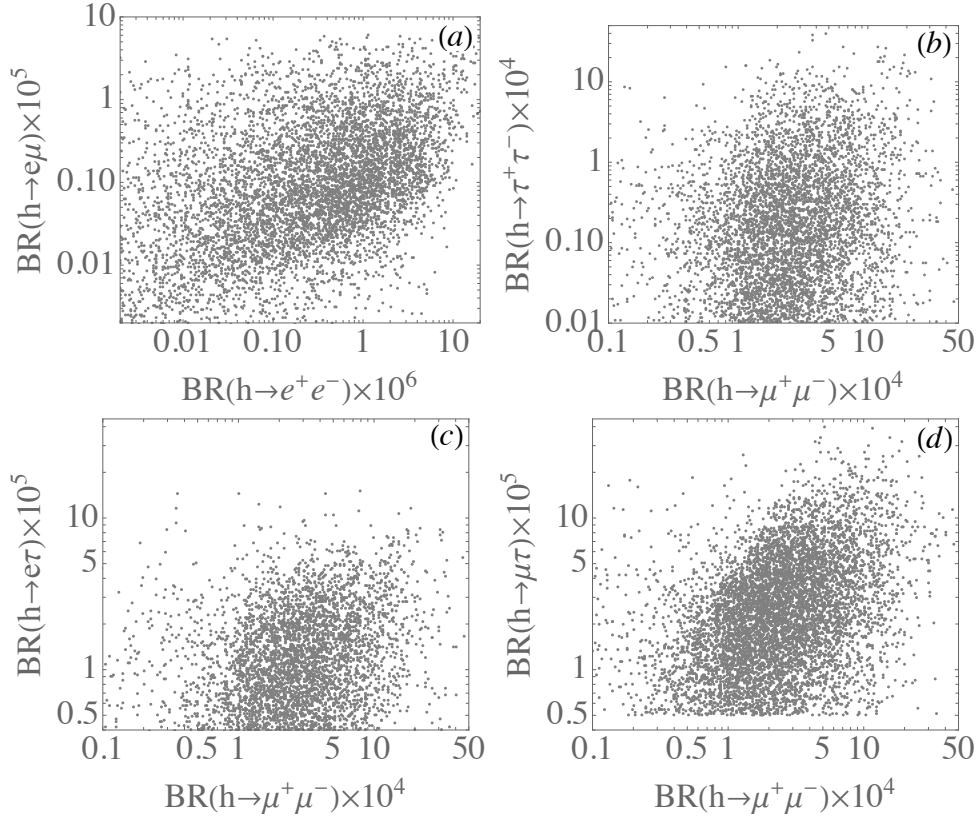


FIG. 10: Scatter plots for the correlations among  $BR(h \rightarrow \ell\ell')$ .

## VI. SUMMARY

To explore possible mechanisms to enhance the top-FCNC and LFV processes, which are highly suppressed in the SM, we extend the SM by imposing a  $Z_2$  symmetry and introducing an inert Higgs doublet, a singlet charged Higgs boson, and a singlet vector-like quark and



neutral leptons. It has been found that the enhancement of the top-FCNC decays has to rely on the Yukawa couplings of  $\mathcal{O}(1)$ . Since the new Higgs trilinear couplings  $h-H_I^\pm-\chi^\mp$  appear and their magnitudes can be much larger than the gauge couplings of electroweak interactions, the BR for the loop-induced  $t \rightarrow ch$  can reach  $\mathcal{O}(10^{-4})$  in the model and  $t \rightarrow cZ$  is of  $\mathcal{O}(10^{-5})$ , though the BR for  $t \rightarrow c\gamma$  stays below  $10^{-6}$ .

To satisfy the strict limit from  $\mu \rightarrow e\gamma$ , we simply set  $BR(\mu \rightarrow e\gamma) \approx 0$  to make the parameter scan more efficient. Based on the current upper limits of  $\tau \rightarrow \ell\gamma$  and  $h \rightarrow ee/e\mu$ , it has been found that the BRs for  $h \rightarrow \mu^+\mu^-$  and  $h \rightarrow \tau\tau$  can maximally reach  $\mathcal{O}(10^{-3})$ , with the former possibly having a somewhat larger BR. In addition, the resulting  $BR(h \rightarrow \mu\tau)$  of  $\mathcal{O}(10^{-4})$  can be within the sensitivity of HL-LHC.

The lepton  $g-2$  generally can be either positive or negative in the model. Using the constrained parameters, it is found that the predicted muon  $g-2$  can match the experimental result within  $2\sigma$  errors, where the hadronic vacuum polarization in the SM is obtained by the data-driven approach. Moreover, because the involved Yukawa couplings are different from those in the muon  $g-2$ , the sign of electron  $g-2$  in the model is not fixed. Nevertheless, its magnitude can be consistent with the observed values in different atomic systems that are of opposite signs.

## Acknowledgments

This work was supported in part by the National Science and Technology Council, Taiwan under the Grant No. MOST-110-2112-M-006-010-MY2 (C. H. Chen) and Grants No. MOST-108-2112-M-002-005-MY3 and No. 111-2112-M-002-018-MY3 (C. W. Chiang and C. -W. Su).

- 
- [1] S. L. Glashow, J. Iliopoulos and L. Maiani, Phys. Rev. D **2**, 1285 (1970).
  - [2] J. A. Aguilar-Saavedra, Acta Phys. Polon. B **35**, 2695 (2004) [hep-ph/0409342].
  - [3] G. Abbas, A. Celis, X. Q. Li, J. Lu and A. Pich, JHEP **1506**, 005 (2015) [arXiv:1503.06423 [hep-ph]].
  - [4] S. Balaji, Phys. Rev. D **102** (2020) no.11, 113010 [arXiv:2009.03315 [hep-ph]].

- [5] P. Azzi, S. Farry, P. Nason, A. Tricoli, D. Zeppenfeld, R. Abdul Khalek, J. Alimena, N. Andari, L. Aperio Bella and A. J. Armbruster, *et al.* CERN Yellow Rep. Monogr. **7**, 1-220 (2019) [arXiv:1902.04070 [hep-ph]].
- [6] M. Cepeda, S. Gori, P. Ilten, M. Kado, F. Riva, R. Abdul Khalek, A. Aboubrahim, J. Alimena, S. Alioli and A. Alves, *et al.* CERN Yellow Rep. Monogr. **7**, 221-584 (2019) [arXiv:1902.00134 [hep-ph]].
- [7] A. M. Baldini *et al.* [MEG II], Eur. Phys. J. C **78**, no.5, 380 (2018) [arXiv:1801.04688 [physics.ins-det]].
- [8] E. Kou *et al.* [Belle-II], PTEP **2019**, no.12, 123C01 (2019) [erratum: PTEP **2020**, no.2, 029201 (2020)] [arXiv:1808.10567 [hep-ex]].
- [9] K. J. Abraham, K. Whisnant, J. M. Yang and B. L. Young, Phys. Rev. D **63**, 034011 (2001) [hep-ph/0007280].
- [10] G. Eilam, A. Gemintern, T. Han, J. M. Yang and X. Zhang, Phys. Lett. B **510**, 227 (2001) [hep-ph/0102037].
- [11] J. A. Aguilar-Saavedra, Phys. Rev. D **67**, 035003 (2003) Erratum: [Phys. Rev. D **69**, 099901 (2004)] [hep-ph/0210112].
- [12] U. K. Dey and T. Jha, Phys. Rev. D **94** (2016) no.5, 056011 [arXiv:1602.03286 [hep-ph]].  
Copy to ClipboardDownload
- [13] R. Gaitan, R. Martinez, J. H. M. de Oca and E. A. Garces, Phys. Rev. D **98**, no. 3, 035031 (2018) [arXiv:1710.04262 [hep-ph]].
- [14] M. Badziak and K. Harigaya, Phys. Rev. Lett. **120** (2018) no.21, 211803 [arXiv:1711.11040 [hep-ph]].
- [15] J. F. Shen, Y. Q. Li and Y. B. Liu, Phys. Lett. B **776**, 391-395 (2018) [arXiv:1712.03506 [hep-ph]].
- [16] C. W. Chiang, U. K. Dey and T. Jha, Eur. Phys. J. Plus **134**, no.5, 210 (2019) [arXiv:1807.01481 [hep-ph]].
- [17] K. Y. Oyulmaz, A. Senol, H. Denizli, A. Yilmaz, I. Turk Cakir and O. Cakir, Eur. Phys. J. C **79**, no.1, 83 (2019) [arXiv:1811.01074 [hep-ph]].
- [18] C. H. Chen and T. Nomura, Eur. Phys. J. C **79**, no.8, 644 (2019) [arXiv:1812.05904 [hep-ph]].
- [19] M. A. Arroyo-Ureña, R. Gaitán, E. A. Herrera-Chacón, J. H. Montes de Oca Y. and T. A. Valencia-Pérez, JHEP **07**, 041 (2019) [arXiv:1903.02718 [hep-ph]].

- [20] L. Shi and C. Zhang, Chin. Phys. C **43**, no.11, 113104 (2019) [arXiv:1906.04573 [hep-ph]].
- [21] Y. B. Liu and S. Moretti, Phys. Rev. D **101**, no.7, 075029 (2020) [arXiv:2002.05311 [hep-ph]].
- [22] W. S. Hou, T. H. Hsu and T. Modak, Phys. Rev. D **102**, no.5, 055006 (2020) [arXiv:2008.02573 [hep-ph]].
- [23]
- [23] S. Y. Bie, G. L. Liu and W. Wang, Chin. Phys. C **45**, no.1, 013106 (2021) [arXiv:2009.04858 [hep-ph]].
- [24] P. Gutierrez, R. Jain and C. Kao, Phys. Rev. D **103**, no.11, 115020 (2021) [arXiv:2012.09209 [hep-ph]].
- [25] Y. Liu, B. Yan and R. Zhang, Phys. Lett. B **827**, 136964 (2022) [arXiv:2103.07859 [hep-ph]].
- [26] F. M. Cai, S. Funatsu, X. Q. Li and Y. D. Yang, [arXiv:2202.08091 [hep-ph]].
- [27] A. I. Hernández-Juárez and G. Tavares-Velasco, [arXiv:2203.16819 [hep-ph]].
- [28] C. H. Chen and T. Nomura, Phys. Rev. D **106**, no.9, 095005 (2022) [arXiv:2204.01214 [hep-ph]].
- [29] G. W. Bennett *et al.* [Muon g-2], Phys. Rev. D **73**, 072003 (2006) [arXiv:hep-ex/0602035 [hep-ex]].
- [30] B. Abi *et al.* [Muon g-2], Phys. Rev. Lett. **126**, no.14, 141801 (2021) [arXiv:2104.03281 [hep-ex]].
- [31] C. T. H. Davies *et al.* [Fermilab Lattice, LATTICE-HPQCD and MILC], Phys. Rev. D **101**, no.3, 034512 (2020) [arXiv:1902.04223 [hep-lat]].
- [32] S. Borsanyi, Z. Fodor, J. N. Guenther, C. Hoelbling, S. D. Katz, L. Lellouch, T. Lippert, K. Miura, L. Parato and K. K. Szabo, *et al.*, Nature **593**, no.7857, 51-55 (2021) [arXiv:2002.12347 [hep-lat]].
- [33] R. H. Parker, Yu. Chenghui, W. Zhong, B. Estey, H. Müller, Science **360**, 191 (2018).
- [34] L. Morel, Z. Yao, P. Cladé, S. Guellati-Khélifa, Nature **588** (7836), 61-65 (2020).
- [35] C. H. Chen and C. Q. Geng, Phys. Lett. B **511**, 77-84 (2001) [arXiv:hep-ph/0104151 [hep-ph]].
- [36] C. H. Chen, T. Nomura and H. Okada, Phys. Lett. B **774**, 456-464 (2017) [arXiv:1703.03251 [hep-ph]].
- [37] C. H. Chen and T. Nomura, Phys. Rev. D **100**, no.1, 015024 (2019) [arXiv:1903.03380 [hep-ph]].

- [38] C. H. Chen and T. Nomura, JHEP **09**, 090 (2021) [arXiv:2001.07515 [hep-ph]].
- [39] C. H. Chen and T. Nomura, Nucl. Phys. B **964**, 115314 (2021) [arXiv:2003.07638 [hep-ph]].
- [40] K. F. Chen, C. W. Chiang and K. Yagyu, JHEP **09**, 119 (2020) [arXiv:2006.07929 [hep-ph]].
- [41] I. Doršner, S. Fajfer and S. Saad, Phys. Rev. D **102**, no.7, 075007 (2020) [arXiv:2006.11624 [hep-ph]].
- [42] S. Jana, P. K. Vishnu, W. Rodejohann and S. Saad, Phys. Rev. D **102**, no.7, 075003 (2020) [arXiv:2008.02377 [hep-ph]].
- [43] E. J. Chun and T. Mondal, JHEP **11**, 077 (2020) [arXiv:2009.08314 [hep-ph]].
- [44] S. P. Li, X. Q. Li, Y. Y. Li, Y. D. Yang and X. Zhang, JHEP **01**, 034 (2021) [arXiv:2010.02799 [hep-ph]].
- [45] A. Bodas, R. Coy and S. J. D. King, Eur. Phys. J. C **81**, no.12, 1065 (2021) [arXiv:2102.07781 [hep-ph]].
- [46] M. J. Baker, P. Cox and R. R. Volkas, JHEP **05**, 174 (2021) [arXiv:2103.13401 [hep-ph]].
- [47] C. W. Chiang and K. Yagyu, Phys. Rev. D **103**, no.11, L111302 (2021) [arXiv:2104.00890 [hep-ph]].
- [48] C. H. Chen, C. W. Chiang and T. Nomura, Phys. Rev. D **104**, no.5, 055011 (2021) [arXiv:2104.03275 [hep-ph]].
- [49] J. L. Yang, H. B. Zhang, C. X. Liu, X. X. Dong and T. F. Feng, JHEP **08**, 086 (2021) [arXiv:2104.03542 [hep-ph]].
- [50] P. Athron, C. Balázs, D. H. J. Jacob, W. Kotlarski, D. Stöckinger and H. Stöckinger-Kim, JHEP **09**, 080 (2021) [arXiv:2104.03691 [hep-ph]].
- [51] P. Escribano, J. Terol-Calvo and A. Vicente, Phys. Rev. D **103**, no.11, 115018 (2021) [arXiv:2104.03705 [hep-ph]].
- [52] J. Y. Cen, Y. Cheng, X. G. He and J. Sun, Nucl. Phys. B **978**, 115762 (2022) [arXiv:2104.05006 [hep-ph]].
- [53] D. Borah, M. Dutta, S. Mahapatra and N. Sahu, Phys. Lett. B **820**, 136577 (2021) [arXiv:2104.05656 [hep-ph]].
- [54] A. Jueid, J. Kim, S. Lee and J. Song, Phys. Rev. D **104**, no.9, 095008 (2021) [arXiv:2104.10175 [hep-ph]].
- [55] A. Dey, J. Lahiri and B. Mukhopadhyaya, Phys. Rev. D **106**, no.5, 055023 (2022) [arXiv:2106.01449 [hep-ph]].

- [56] S. Li, Y. Xiao and J. M. Yang, Eur. Phys. J. C **82**, no.3, 276 (2022) [arXiv:2107.04962 [hep-ph]].
- [57] L. T. Hue, A. E. Cárcamo Hernández, H. N. Long and T. T. Hong, Nucl. Phys. B **984**, 115962 (2022) [arXiv:2110.01356 [hep-ph]].
- [58] C. W. Chiang, R. Obuchi and K. Yagyu, JHEP **05**, 070 (2022) [arXiv:2202.07784 [hep-ph]].
- [59] T. A. Chowdhury, M. Ehsanuzzaman and S. Saad, JCAP **08**, 076 (2022) [arXiv:2203.14983 [hep-ph]].
- [60] S. Li, Z. Li, F. Wang and J. M. Yang, Nucl. Phys. B **983**, 115927 (2022) [arXiv:2205.15153 [hep-ph]].
- [61] S. Arora, M. Kashav, S. Verma and B. C. Chauhan, [arXiv:2206.12828 [hep-ph]].
- [62] T. Aaltonen *et al.* [CDF], Science **376**, no.6589, 170-176 (2022).
- [63] M. Aaboud *et al.* [ATLAS], Eur. Phys. J. C **78**, no.2, 110 (2018) [erratum: Eur. Phys. J. C **78**, no.11, 898 (2018)] [arXiv:1701.07240 [hep-ex]].
- [64] T. A. Aaltonen *et al.* [CDF and D0], Phys. Rev. D **88**, no.5, 052018 (2013) [arXiv:1307.7627 [hep-ex]].
- [65] S. Heinemeyer, W. Hollik, G. Weiglein and L. Zeune, JHEP **12**, 084 (2013) [arXiv:1311.1663 [hep-ph]].
- [66] A. Strumia, JHEP **08**, 248 (2022) doi:10.1007/JHEP08(2022)248 [arXiv:2204.04191 [hep-ph]].
- [67] E. Bagnaschi, J. Ellis, M. Madigan, K. Mimasu, V. Sanz and T. You, JHEP **08**, 308 (2022) [arXiv:2204.05260 [hep-ph]].
- [68] H. Bahl, J. Braathen and G. Weiglein, Phys. Lett. B **833**, 137295 (2022) [arXiv:2204.05269 [hep-ph]].
- [69] Y. Cheng, X. G. He, Z. L. Huang and M. W. Li, Phys. Lett. B **831**, 137218 (2022) [arXiv:2204.05031 [hep-ph]].
- [70] P. Asadi, C. Cesarotti, K. Fraser, S. Homiller and A. Parikh, [arXiv:2204.05283 [hep-ph]].
- [71] A. Crivellin, M. Kirk, T. Kitahara and F. Mescia, Phys. Rev. D **106**, no.3, L031704 (2022) [arXiv:2204.05962 [hep-ph]].
- [72] P. Fileviez Perez, H. H. Patel and A. D. Plascencia, Phys. Lett. B **833**, 137371 (2022) doi:10.1016/j.physletb.2022.137371 [arXiv:2204.07144 [hep-ph]].
- [73] S. Kanemura and K. Yagyu, Phys. Lett. B **831**, 137217 (2022)

- doi:10.1016/j.physletb.2022.137217 [arXiv:2204.07511 [hep-ph]].
- [74] J. Kim, S. Lee, P. Sanyal and J. Song, Phys. Rev. D **106**, no.3, 035002 (2022) doi:10.1103/PhysRevD.106.035002 [arXiv:2205.01701 [hep-ph]].
  - [75] X. Q. Li, Z. J. Xie, Y. D. Yang and X. B. Yuan, [arXiv:2205.02205 [hep-ph]].
  - [76] R. Dacruz and A. Thapa, [arXiv:2205.02217 [hep-ph]].
  - [77] T. A. Chowdhury and S. Saad, Phys. Rev. D **106**, no.5, 055017 (2022) [arXiv:2205.03917 [hep-ph]].
  - [78] J. Gao, D. Liu and K. Xie, [arXiv:2205.03942 [hep-ph]].
  - [79] Y. Cheng, X. G. He, F. Huang, J. Sun and Z. P. Xing, [arXiv:2208.06760 [hep-ph]].
  - [80] R. Barbieri, L. J. Hall and V. S. Rychkov, Phys. Rev. D **74**, 015007 (2006) [arXiv:hep-ph/0603188 [hep-ph]].
  - [81] A. Zee, Phys. Lett. B **93**, 389 (1980) [erratum: Phys. Lett. B **95**, 461 (1980)]
  - [82] C. H. Chen, C. W. Chiang, T. Nomura and C. W. Su, JHEP **09**, 166 (2022) [arXiv:2201.10759 [hep-ph]].
  - [83] J. de Blas, M. Pierini, L. Reina and L. Silvestrini, [arXiv:2204.04204 [hep-ph]].
  - [84] K. G. Klimenko, Theor. Math. Phys. **62**, 58-65 (1985).
  - [85] K. Kannike, Eur. Phys. J. C **72**, 2093 (2012) [arXiv:1205.3781 [hep-ph]].
  - [86] R. Longas, D. Portillo, D. Restrepo and O. Zapata, JHEP **03** (2016), 162 [arXiv:1511.01873 [hep-ph]].
  - [87] B. W. Lee, C. Quigg and H. B. Thacker, Phys. Rev. D **16**, 1519 (1977).
  - [88] W. Grimus, L. Lavoura, O. M. Ogreid and P. Osland, Nucl. Phys. B **801** (2008), 81-96 [arXiv:0802.4353 [hep-ph]].
  - [89] M. E. Peskin and T. Takeuchi, Phys. Rev. Lett. **65** (1990), 964-967.
  - [90] M. E. Peskin and T. Takeuchi, Phys. Rev. D **46** (1992), 381-409.
  - [91] I. Maksymyk, C. P. Burgess and D. London, Phys. Rev. D **50** (1994), 529-535 [arXiv:hep-ph/9306267 [hep-ph]].
  - [92] J. Herrero-García, T. Ohlsson, S. Riad and J. Wirén, JHEP **04** (2017), 130 [arXiv:1701.05345 [hep-ph]].
  - [93] A. Lenz, U. Nierste, J. Charles, S. Descotes-Genon, A. Jantsch, C. Kaufhold, H. Lacker, S. Monteil, V. Niess and S. T’Jampens, Phys. Rev. D **83** (2011), 036004 [arXiv:1008.1593 [hep-ph]].

- [94] R. L. Workman *et al.* [Particle Data Group], PTEP **2022** (2022) no.8, 083C01
- [95] A. Castillo, R. A. Diaz and J. Morales, Int. J. Mod. Phys. A **29**, no.18, 1450085 (2014) [arXiv:1309.0831 [hep-ph]].
- [96] G. Aad *et al.* [ATLAS], JHEP **04**, 165 (2021) [arXiv:2102.01444 [hep-ex]].
- [97] A. Pierce and J. Thaler, JHEP **08**, 026 (2007) [arXiv:hep-ph/0703056 [hep-ph]].
- [98] E. Lundstrom, M. Gustafsson and J. Edsjo, Phys. Rev. D **79**, 035013 (2009) [arXiv:0810.3924 [hep-ph]].
- [99] M. Merchand and M. Sher, JHEP **03**, 108 (2020) [arXiv:1911.06477 [hep-ph]].
- [100] G. Belanger, A. Mjallal and A. Pukhov, Phys. Rev. D **105**, no.3, 035018 (2022) [arXiv:2108.08061 [hep-ph]].
- [101] G. Aad *et al.* [ATLAS], Eur. Phys. J. C **82**, no.4, 334 (2022) [arXiv:2112.01302 [hep-ex]].
- [102] D. de Florian *et al.* [LHC Higgs Cross Section Working Group], [arXiv:1610.07922 [hep-ph]].